Antiferromagnetic order enhanced by local dissipation

Oscar Bouverot-Dupuis,[1,2] Saptarshi Majumdar [●],[1,2] Alberto Rosso,[1] and Laura Foini[2]

[1]*Université Paris Saclay, CNRS, LPTMS, 91405, Orsay, France*

[2]*IPhT, CNRS, CEA, Université Paris Saclay, 91191 Gif-sur-Yvette, France*

We study an XXZ spin chain at zero magnetization coupled to a collection of local harmonic baths at zero temperature. We map this system on a $(1 + 1)$D effective field theory using bosonization, where the effect of the bath is taken care of in an exact manner. We provide analytical and numerical evidence of the existence of two phases at zero temperature: a Luttinger liquid (LL) and an antiferromagnetic phase (AFM), separated by a phase transition akin to the Berezinsky–Kosterlitz–Thouless type. While the bath is responsible for the LL-AFM transition for subohmic baths, the LL-AFM transition for superohmic baths is due to the interactions within the spin chain.

I. INTRODUCTION

The problem of a quantum-mechanical system interacting with an environment is ubiquitous in physics. These interactions can originate from a surrounding bath, an external driving force, an optical or solid lattice, or something else. Regardless, the resulting behavior of the system coupled to its environment can drastically differ from that of the isolated system. At one end of the spectrum, if the environment evolves on timescales much larger than that of the system, it is said to be frozen. In the case where the environment settles in a random frozen state, it can be accurately modeled by quenched disorder. This is the case of the celebrated Anderson model [1], where a particle gets localized due to the presence of a random potential, leading to vanishing transport properties. The other end of the spectrum corresponds to environments with very rapid dynamics that can safely be considered Markovian and for which the Lindblad master equation has proven very useful [2]. In between these two timescales are slowly varying baths for which a successful quantum formulation was established by Caldeira and Leggett [3,4]. They studied a single degree of freedom (spin or particle) coupled to a bath, such as the spin-boson model [5] or a quantum Brownian particle in a periodic potential [6,7]. In these models, the system is coupled to a bath of phonons that is simple enough to be traced over and recover effective dynamics for the system of interest.

More recently, interest has started shifting towards many-body versions of these models. Going from one particle to many opens the door to another zoology of phenomena, but some single-particle effects can also persist. For instance, adding interactions to the Anderson model is conjectured to preserve localization at finite temperature through the so-called many-body localization (MBL) [8–10], i.e., the fact that some isolated many-body systems can fail to reach equilibrium and retain a memory of their initial conditions.

In this paper, we study the well-known XXZ spin chain coupled to local baths of harmonic oscillators (see Fig. 1). To a certain extent, this model can be viewed as a many-body

extension in $(1 + 1)$D of the spin-boson model in $(0+1)$D [5,11], or an extension of the most studied many-body localization setup, an XXZ spin chain in a random magnetic field [8], where the fields are now replaced by local baths. The effect of the bath on its corresponding spin can be captured by an exponent s (see the next section for a more formal definition) which allows us to model a large variety of baths. For a spin chain at finite magnetization and any s, it has been shown that the bath induces fractional excitations that create a dissipative phase presenting signatures of localization [12–15]. At zero magnetization, the only known results are for $s = 1$, i.e., an ohmic bath, for which a superfluid to insulator transition has been proposed in Refs. [15,16]. In this paper, we broaden the scope of these studies by focusing on the zero magnetization case and allowing for a generic exponent s. Our results show the existence of a Berezinsky–Kosterlitz–Thouless (BKT) phase transition between a Luttinger liquid (LL) and an antiferromagnetic (AFM) phase. The exact location of the transition point depends on the bath exponent s and is shifted compared to the non-dissipative spin chain for $s < 1$.

The paper is organized as follows: Section II introduces the model and maps it to a bosonic effective field theory. Section III then presents a clear overview of the main results in terms of this effective field-theoretic description. These results were derived using thorough numerical and analytical approaches. On the analytical side, a perturbative renormalization group study is presented in Sec. IV and is complemented by a variational approach in Sec. V. These analytical predictions are then tested for several observables against an exact numerical simulation of the field theory in Sec. VI. Finally, a brief discussion of the results and concluding remarks are made in Sec. VII. Unless specified otherwise (as in Sec. V), the zero temperature ($\beta \to \infty$) and thermodynamic ($L \to \infty$) limits will always be understood.

II. MODEL

The XXZ spin chain is a 1D periodic chain of N spins, total length L, and lattice spacing $a = \frac{L}{N}$. It evolves according
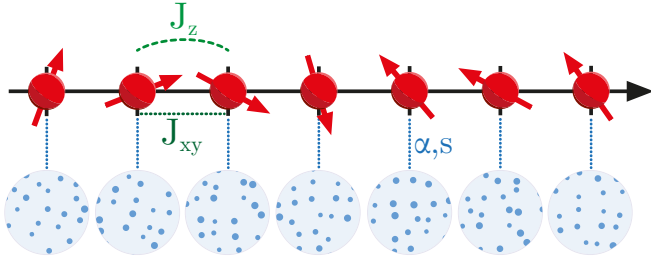
FIG. 1. Schematic representation of the model. An XXZ spin chain with parameters J_z, J_{xy} has its spins coupled to independent and identical collections of harmonic oscillators. The spin-bath interaction is assumed to be fully described by the parameters α and s.

to the Hamiltonian

$$H_S = \sum_{j=1}^{N} J_z S_j^z S_{j+1}^z - J_{xy}\left(S_j^x S_{j+1}^x + S_j^y S_{j+1}^y\right), \quad (1)$$

where S_i^μ are the spin-1/2 operators. Each spin is then coupled to a set of quantum harmonic oscillators by

$$H_{SB} = \sum_{j=1}^{N} S_j^z \sum_k \lambda_k X_{k,j}, \quad (2)$$

and the oscillators' Hamiltonian is

$$H_B = \sum_{j=1}^{N} \sum_k \frac{P_{k,j}^2}{2m_k} + \frac{1}{2}m_k\Omega_k^2 X_{k,j}^2. \quad (3)$$

Hence the total Hamiltonian of the dissipative system $H = H_S + H_{SB} + H_B$. Note that the baths are local, i.e., each bath has its independent spin that it acts upon and the baths are not spatially correlated. Thus, its effect can be thought of as an instance of annealed disorder $h_j(t) = \sum_k \lambda_k X_{k,j}$, acting locally through $H_{SB} = \sum_{j=1}^{N} h_j(t) S_j^z$. The quenched limit of this problem $h_j(t) = h_j$ has already been studied in Refs. [17–19], where a zero-temperature delocalization-localization transition was found. Other bath-spin couplings are also possible and have been studied in, for example, Refs. [20,21].

A common tool to study such many-body systems is the Lindblad master equation [2], which makes use of a Markovian approximation of the bath's dynamics. Nevertheless, in this paper, we will not use it and resort to an approach similar to that of Leggett *et al.* [5], which takes the bath into account in an exact manner. Following the idea of Ref. [5], the bath characteristics are completely encoded in the spectral function

$$J(\Omega) = \frac{\pi}{2} \sum_k \frac{\lambda_k^2}{\Omega_k m_k} \delta(\Omega - \Omega_k), \quad (4)$$

which we assume to have the low-energy behavior

$$J(\Omega) = \alpha \frac{\pi \Omega_D^{1-s}}{\Gamma(1+s)} \Omega^s \quad \text{for} \quad \Omega \in [0, \Omega_D], \quad (5)$$

where s is the bath exponent and α measures the strength of the coupling to the bath. Following the classification from Leggett *et al.*, we call $s = 1$ an ohmic bath, while $0 < s < 1$ is a subohmic bath and $s > 1$ is a superohmic bath. The rest

of this section will be dedicated to deriving an effective action for our system using the bosonization technique.

A. Bosonization

To implement the bosonization procedure described in Refs. [12,22,23], one must first map the spin chain to a one-dimensional spinless fermionic system using the Jordan–Wigner transformation. With the usual notations c_j, $c_j^\dagger$ for the ladder operators and $n_j = c_j^\dagger c_j$, the XXZ spin chain Hamiltonian becomes $H_S = H_{xy} + H_z$, where

$$H_{xy} = -\frac{J_{xy}}{2} \sum_{j=1}^{N} (c_{j+1}^\dagger c_j + c_j^\dagger c_{j+1}), \quad (6)$$

$$H_z = \sum_{j=1}^{N} J_z\left(n_j - \frac{1}{2}\right)\left(n_{j+1} - \frac{1}{2}\right). \quad (7)$$

The hopping Hamiltonian H_{xy} can be diagonalized in Fourier space as $H_{xy} = \sum_k \varepsilon_k c_k^\dagger c_k$ with $\varepsilon_k = -J_{xy}\cos(ka)$. In the rest of the paper, we will consider the spin chain to be at zero magnetization, which corresponds to a half-filled fermionic chain and a Fermi momentum $k_F = \frac{\pi}{2a}$ that is commensurate with the lattice spacing a. The application of the bosonization technique then requires linearizing the spectrum ε_k around k_F, which leads to a field-theoretic description of the Hamiltonian H_S with the action $S_S = S_{LL} + S_g$, given by

$$S_{LL} = \int \frac{dx\,d\tau}{2\pi K}\left[u(\partial_x\phi(x,\tau))^2 + \frac{1}{u}(\partial_\tau\phi(x,\tau))^2\right], \quad (8)$$

$$S_g = -\frac{gu}{2\pi^2 a^2} \int dx\,d\tau \cos[4\phi(x,\tau)], \quad (9)$$

where $x \in [0, L]$ denotes the spatial coordinate, $\tau \in [0, \beta]$ is the imaginary time coordinate with β the inverse temperature of the system, and S_{LL} describes a LL. The parameters u, K are the so-called Luttinger parameters and, with g, are related to the microscopic parameters. The Bethe ansatz gives their exact expressions for the spin chain without dissipation [e.g., $K_{Bethe}^{-1} = \frac{2}{\pi}\arccos(-J_z/J_{xy})$] while the bosonization yields approximate expressions valid in the $J_z \ll J_{xy}$ limit (e.g., $K_{bosonization}^{-1} = \sqrt{1 + \frac{4J_z}{\pi J_{xy}}}$) (see Appendix A for more details). On top of this description of the isolated spin chain, one needs to add the effect of the bath captured by $H_{SB} + H_B$. This requires the bosonized expression of S_j^z:

$$S_j^z = -\frac{a}{\pi}\nabla\phi(x_j) + \frac{(-1)^j}{\pi}\cos[2\phi(x_j)], \quad x_j = ja. \quad (10)$$

Using this expression to write a path integral representation of $H_B + H_{SB}$, one realizes that the bath degrees of freedom are quadratic and can therefore be integrated out. This leads to the following additional term in the action:

$$S_\alpha = -\frac{a}{2\pi^2} \int dx\,d\tau\,d\tau'$$

$$\times \left[\partial_x\phi(x,\tau) - \frac{(-1)^{x/a}}{a}\cos[2\phi(x,\tau)]\right]\mathcal{D}(\tau,\tau')$$

$$\times \left[\partial_x\phi(x,\tau') - \frac{(-1)^{x/a}}{a}\cos[2\phi(x,\tau')]\right], \quad (11)$$

where one has to keep in mind the underlying lattice coordinates $x_j = ja$ to make sense of the term $(-1)^{x/a}$ which arises from the commensurability of the excitation wavelength with the lattice spacing. One can show using the spectral function $J(\Omega)$ that the dissipative kernel is $\mathcal{D}(\tau, \tau') \sim \alpha \tau_c^{s-1} |\tau - \tau'|^{-1-s}$ for $\tau > \tau_c = 1/\Omega_D$ (see Appendix B for the detailed computation). For the sake of simplicity, we relate the imaginary-time and space cutoffs as $a = u\tau_c$ which doesn't change the underlying physics. Equation (11) can be further simplified by dropping the rapidly fluctuating terms $(-1)^{x/a} \partial_x \phi(x, \tau) \cos[2\phi(x, \tau')]$, and the cross gradient term $\partial_x \phi(x, \tau) \partial_x \phi(x, \tau')$, which is irrelevant by power counting. The total bosonized action $S = S_{\text{LL}} + S_g + S_\alpha$ is thus

$$
S = \int \frac{dxd\tau}{2\pi K} \left[u(\partial_x \phi(x, \tau))^2 + \frac{1}{u}(\partial_\tau \phi(x, \tau))^2 \right]
$$
$$
- \frac{g}{2\pi^2} \int \frac{dxd\tau}{a\tau_c} \cos[4\phi(x, \tau)]
$$
$$
- \frac{\alpha}{2\pi^2} \int_{|\tau-\tau'|>\tau_c} \frac{dxd\tau d\tau'}{a\tau_c^{1-s}} \frac{\cos[2\phi(x, \tau)] \cos[2\phi(x, \tau')]}{|\tau - \tau'|^{1+s}}. \quad (12)
$$

This effective action is that of a LL with two types of interactions: a local sine-Gordon interaction controlled by g and a long-range interaction controlled by α, which is commonly encountered in generalized XY models [24,25] or dissipative quantum systems [26–28]. Note that the long-range interaction involving $\cos[2\phi(x, \tau)] \cos[2\phi(x, \tau')]$ can be rewritten as the sum of $\cos[2(\phi(x, \tau) + \phi(x, \tau'))]$ and $\cos[2(\phi(x, \tau) - \phi(x, \tau'))]$. In the case of an incommensurate XXZ spin chain [12–14], only the latter term remains and the sine-Gordon term vanishes. It has been shown that this term gives rise to fractional excitations $|\omega_n|^s$ in the spectrum of the incommensurate spin chain. However, from our variational analysis in Sec. V, we will demonstrate that this fractional term is absent from our commensurate model and is replaced by a gap.

III. MAIN RESULTS

From the bosonized action in Eq. (12), the analytical and numerical tools used in the following sections infer the zero temperature ($\beta \to \infty$) and thermodynamic ($L \to \infty$) phase diagram depicted in Fig. 2. A LL and an AFM are separated by a transition that depends on the bath exponent s.

(1) For a superohmic bath ($s > 1$), a standard BKT transition [29] occurs at $K_c = 1/2$ (in the limit of infinitesimal α, g) and is driven by the coupling g which comes from the internal interactions of the spin chain. The spin chain is an LL for $K \geqslant K_c$ while it becomes an AFM at $K < K_c$.

(2) For an ohmic bath ($s = 1$), the system undergoes a BKT-like transition at $K_c = 1/2$ (in the limit of infinitesimal α, g) driven by both the coupling g, and the system-bath coupling denoted by the α.

(3) For a subohmic bath ($s < 1$), the coupling α, shifts the BKT-like transition to $K_c = 1 - s/2$ (in the limit of infinitesimal α, g). This increased value of K_c extends the area of the AFM.

In all cases, the critical point K_c increases with α and g. The two phases are characterized as follows. On the one
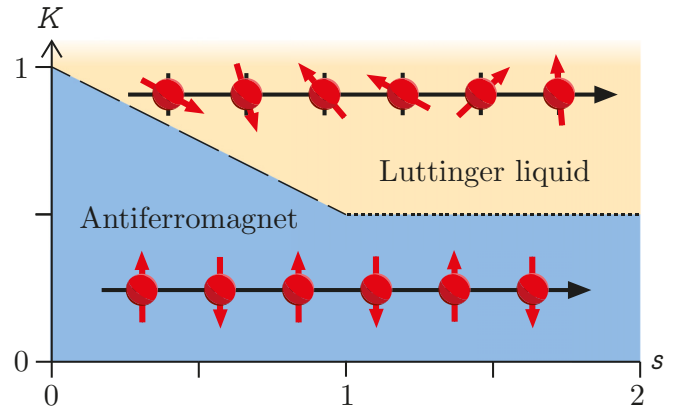

FIG. 2. Phase diagram in the (K, s) plane as described by the RG analysis in Sec. IV and the variational method in Sec. V for infinitesimal value of α and g. The golden-colored phase is a gapless LL, and the blue-colored phase is a gapped AFM phase. Along the dashed line, the phase transition is controlled by the coupling α to the bath, while along the dotted line it is governed by g, which describes the internal interactions of the spin chain.

hand, the LL is a critical phase exhibiting quasi-long range order as seen by the power-law decay of spin-spin correlation functions [22]. On the other hand, the AFM is a gapped (or massive) phase exhibiting long-range order. Although suggested by Ref. [16], we do not find any fractional excitations in the AFM phase, neither from the analytical study nor from the exact numerical simulations. This AFM is of the same nature as the AFM in the sine-Gordon model. The transition admits the (infinite order) order parameter $\langle \cos(2\phi) \rangle$ which is related to the antiferromagnetic spin density wave as $\langle S_j^z \rangle = \frac{(-1)^j}{\pi} \langle \cos(2\phi) \rangle$. We show that $\langle \cos(2\phi) \rangle$ vanishes with the gap of the AFM phase, thus making it an order parameter of the AFM-LL transition.

IV. PERTURBATIVE RENORMALIZATION GROUP APPROACH

Looking at the bosonized action in Eq. (12), we expect that, at large distances and times, the model presents at least two phases: a LL phase where both couplings α and g are irrelevant, and a strongly interacting one where the couplings are relevant. To capture the precise location of the departure from the LL, we implement a perturbative renormalization group (RG) analysis. It turns out it is enough to compute the RG equations up to $O(\alpha, g^2, \alpha g)$ to grasp the interesting physics at play. The perturbative RG analysis was done using the operator product expansion (OPE) formalism [16,30] to respect the real-space sharp cutoff a appearing in the action. The detailed computation can be found in Appendix C and leads to the following RG equations, where the dependence on the renormalization time l has been made explicit:

$$
\frac{d}{dl} \frac{u(l)}{K(l)} = \frac{g(l)^2 u(l)}{\pi^2}, \quad (13)
$$

$$
\frac{d}{dl} \frac{1}{u(l)K(l)} = \frac{2\alpha(l)}{\pi u(l)} + \frac{g(l)^2}{\pi^2 u(l)}, \quad (14)
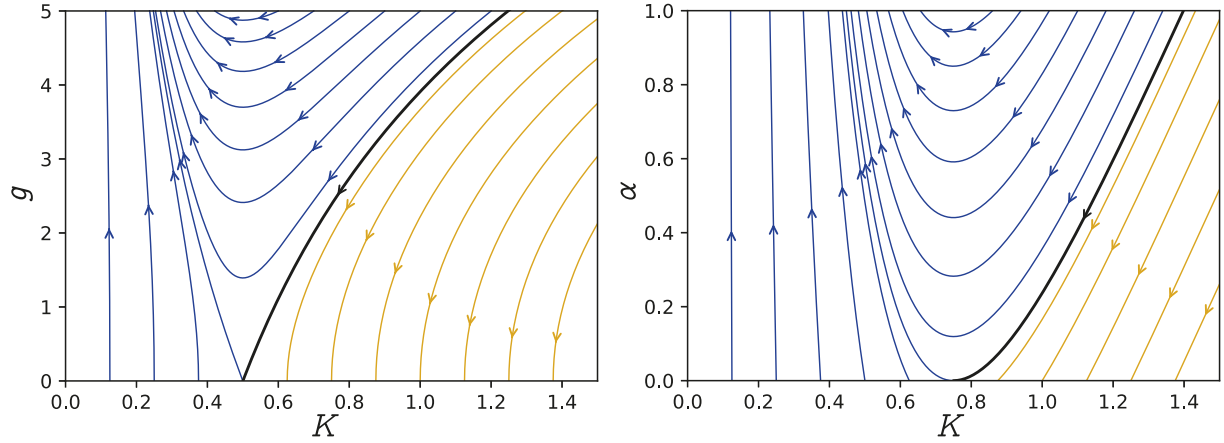$$

FIG. 3. Left: Superohmic transition: RG flow of the couplings g and K according to Eqs. (18) and (19). We distinguish two phases: a Luttinger liquid (LL) depicted in gold and an antiferromagnetic (AFM) phase in blue. The critical point is at $K_c = 1/2$. Right: Subohmic transition (here $s = 0.5$): RG flow of the couplings α and K according to Eqs. (23) and (24). We distinguish two phases: a LL in gold, and an AFM phase in blue. The critical point is at $K_c = 1 - s/2 = 0.75$.

$$\frac{d}{dl}g(l) = (2 - 4K(l))g(l) + \alpha(l), \qquad (15)$$

$$\frac{d}{dl}\alpha(l) = (2 - s - 2K(l))\alpha(l) + \frac{g(l)\alpha(l)}{\pi}, \qquad (16)$$

which agree with and extend [12,16] to generic s. Note how the presence of α in the RG equation for g implies that the bath will generate the coupling g even if its microscopic (bare) value is 0. The symmetric process, i.e., g generates α, is not possible as g can only enhance a nonzero α as seen in Eq. (16). When considering the effect of the bath (i.e., $\alpha \neq 0$), this means that there are not two distinct phase transitions at $K_c = 1/2$ and $K_c = 1 - s/2$ as seen from the scaling dimensions of α and g, but rather a unique transition at $K_c = \max(1 - s/2, 1/2)$. The corresponding phase diagram is depicted in Fig. 2 and shows the existence of a LL for $K > K_c$, with $K_c = 1 - s/2$ for a subohmic bath ($s < 1$) and $K_c = 1/2$ for a superohmic bath ($s > 1$). Note that the long-range cosine potential is irrelevant by power counting for $s > 2$. In this paper, we are interested in understanding the effect of the bath on the system, thus we constrain the value of $s \in [0, 2]$ in Fig. 2.

A. Superohmic bath ($s > 1$)

For a superohmic bath ($s > 1$), near the transition point $K_c = 1/2$, the coupling α has a scaling dimension $2 - s - 2K_c = 1 - s < 0$ which is strongly irrelevant. It can therefore be safely ignored and the RG equations become

$$\frac{d}{dl}u = 0, \qquad (17)$$

$$\frac{d}{dl}\frac{1}{K} = \frac{g^2}{\pi^2}, \qquad (18)$$

$$\frac{d}{dl}g = (2 - 4K)g, \qquad (19)$$

which are the one-loop RG equations of the sine-Gordon model [22,31]. The associated RG flow is shown in Fig. 3 and is known to belong to the BKT universality class. According

to the standard BKT phenomenology, we expect a gap Δ to appear for $K > K_c$. A well-known result derived from the RG equations is that $\Delta \sim \exp(-C(g - g_c)^{-p})$ near the the transition, with $p = 1/2$ [22].

B. Ohmic bath ($s = 1$)

The ohmic bath ($s = 1$) is the most studied type of bath in the literature [12,15,16]. In this setting, the scaling dimensions of α and g both vanish at $K_c = 1/2$, which means the transition is driven by both couplings simultaneously. The RG Eqs. (13)–(16) cannot be simplified any further (as is the case for superohmic or subohmic baths). This leads to an RG flow similar to that of the BKT transition, the main difference being that it is governed by two couplings (α and g) instead of one.

We have shown in Appendix D that this BKT-like transition is characterized by a gap closing as $\Delta \sim \exp(-C(\alpha - \alpha_c)^{-p})$ [or, equivalently, $\exp(-C'(g - g_c)^{-p})$ if one tunes the coupling g instead α] near the transition with $p = \frac{\sqrt{79}+3}{35} \simeq 0.3396$. BKT-like transitions with a parameter $p \neq 1/2$ have been previously found, for example, in the case of 2D melting [32] and long-range Ising models [33]. However, to the best of our knowledge, this particular value of p has not yet been reported in the literature.

C. Subohmic bath ($s < 1$)

For a subohmic bath ($s < 1$), the coupling g is strongly irrelevant near the transition point $K_c = 1 - s/2$ since its scaling dimension is $2 - 4K_c = 2s - 2 < 0$. The RG equations can therefore be simplified by discarding g to give

$$\frac{d}{dl}\frac{u}{K} = 0, \qquad (20)$$

$$\frac{d}{dl}\frac{1}{uK} = \frac{2\alpha}{\pi u}, \qquad (21)$$

$$\frac{d}{dl}\alpha = (2 - s - 2K)\alpha. \qquad (22)$$

The LL action appears to be renormalized along the imaginary-time direction ($\frac{d}{dl}\frac{1}{uK} \neq 0$) but not along the space

direction ($\frac{d}{dl} \frac{u}{K} = 0$) [34]. This anisotropy is due to the long-range interaction in Eq. (12) which only spans the imaginary-time direction. Since the ratio $\frac{u}{K}$ is constant, Eqs. (21) and (22) can be written in terms of K and $\sqrt{\alpha}$ only,

$$\frac{d}{dl} \frac{1}{K} = \frac{\sqrt{\alpha}^2}{\pi}, \tag{23}$$

$$\frac{d}{dl} \sqrt{\alpha} = (1 - s/2 - K)\sqrt{\alpha}, \tag{24}$$

which are exactly the same type of equations as Eqs. (18) and (19), describing the sine-Gordon model. This shows that this phase transition is also BKT-like and doesn't belong to another universality class, as suggested by Ref. [35]. The RG flow associated to these equations is depicted in Fig. 3. Because of the identification with the subohmic RG equations, the gap closes as $\Delta \sim \exp(-C(\alpha - \alpha_c)^{-p})$ near the the transition with $p = 1/2$.

V. VARIATIONAL METHOD

While the perturbative RG is tailored to capture the end of the LL, it fails at describing correctly the physics of the AFM phase. This is why we resort to a variational method *à la* Feynman [22,36] to capture the essential properties of the bulk of the phases. This technique aims at finding an approximate action S_{var} that is very similar to S while being simple enough to allow for analytical computations. We consider a quadratic ansatz

$$S_{\text{var}} = \frac{1}{2} \int \frac{dq}{2\pi} \frac{d\omega_n}{2\pi} \phi^\star(q, \omega_n) G_{\text{var}}^{-1}(q, \omega_n)\phi(q, \omega_n), \tag{25}$$

where $G_{\text{var}}^{-1}(q, \omega_n) = 1/G_{\text{var}}(q, \omega_n)$ is to be determined, $\phi(q, \omega_n)$ is the Fourier transform of $\phi(x, \tau)$ given by $\phi(x, \tau) = \int \frac{dq}{2\pi} \frac{d\omega_n}{2\pi} \phi(q, \omega_n)e^{i(qx - \omega_n\tau)}$, with $\omega_n = \frac{2\pi n}{\beta}$ and $q = \frac{2\pi n}{L}$ the bosonic Matsubara frequencies and the momenta of the system, respectively. The distance from the original action to the variational action is then defined through the variational free energy $F_{\text{var}} = -T \ln Z_{\text{var}} + T \langle S - S_{\text{var}} \rangle_{\text{var}}$ ($\langle \ldots \rangle_{\text{var}}$ stands for the average with respect to S_{var}). Indeed, the true free energy of the original field theory $F = -T \ln Z = T \ln Z_{\text{var}} - T \ln \langle e^{-(S - S_{var})} \rangle_{\text{var}}$, is always upper bounded by F_{var} due to the convexity of the exponential. This defines the best variational action as that which minimizes F_{var}. The goal is thus to solve the vanishing gradient condition $\frac{\delta F_{\text{var}}}{\delta G_{\text{var}}^{-1}(q, \omega_n)} = 0$. It is possible to give an explicit expression for F_{var}, which in turn yields the vanishing gradient equation:

$$G_{\text{var}}^{-1}(q, \omega_n) = \frac{1}{\pi K} \left[uq^2 + \frac{\omega_n^2}{u} \right] + \frac{8g}{\pi^2 a\tau_c} \exp\left[-\frac{2}{\pi^2} \int dq' d\omega_n' G_{\text{var}}(q', \omega_n') \right]$$

$$+ \frac{2\alpha}{\pi^2 a\tau_c^{1-s}} \int_{\tau_c}^\infty \frac{d\tau}{\tau^{1+s}} \sum_{\varepsilon = \pm 1} (1 + \varepsilon \cos \omega_n \tau) \exp\left[-\frac{1}{\pi^2} \int dq' d\omega_n'(1 + \varepsilon \cos \omega_n' \tau) G_{\text{var}}(q', \omega_n') \right]. \tag{26}$$

A. Phase diagram at infinitesimal coupling

In the absence of interactions, i.e., $\alpha = g = 0$, Eq. (26) reduces to $G_{\text{LL}}^{-1}(q, \omega_n) = \frac{1}{\pi K} \left[\frac{\omega_n^2}{u} + uq^2 \right]$ which is just the propagator of the Luttinger liquid. When reintroducing the interaction terms, we expect a gap to appear, like in the sine-Gordon model [22], and maybe some fractional excitations, as in Ref, [16], so we postulate the following ansatz for the propagator in the AFM:

$$G_{\text{AFM}}^{-1}(q, \omega_n) = \frac{1}{\pi K} \left[uq^2 + \frac{\omega_n^2}{u} + v|\omega_n|^s + \frac{\Delta^2}{u} \right], \tag{27}$$

where the parameters Δ and v are to be determined. This ansatz is expected to be valid in the $\alpha, g \to 0$ limit, where one can neglect the renormalization of the Luttinger parameters u, K into u_r, K_r (more on this in the next subsection). The first observation we make is that $v = 0$. This can be understood from the fact that the $|\omega_n|^s$ excitations can only come from the bath-dependent α term in Eq. (27), and the $\varepsilon = 1$ contribution exactly cancels out that of $\varepsilon = -1$. It is worth noticing that unlike Ref. [16], where a similar action with an ohmic bath was studied, this means that we do not find any fractional excitation $|\omega_n|^s$ in our system for any s. We now move on to the determination of the gap Δ. Setting $q = 0$, $\omega_n = 0$ in Eq. (26) yields an equation for Δ that can be written as (see

Appendix E for the detailed computation)

$$\frac{(\Delta\tau_c)^{2-4K}}{K} = g\frac{8}{\pi} + \alpha \frac{4e^{2K\gamma_E}}{\pi} \frac{(\Delta\tau_c)^{s-2K} - 1}{2K - s}, \tag{28}$$

where τ_c is the imaginary-time UV cutoff, and γ_E is Euler's gamma constant. As usual with this variational approach, Eq. (28) is valid deep in the AFM phase where $g, \alpha \ll K_c - K$ [22] and in the limit of small $\Delta\tau_c$. To arrive at the phase diagram shown in Fig. 2, we write Eq. (28) as $\Delta^{2-4K} = a_1 + a_2 \frac{\Delta^{s-2K}}{2K-s}$ with a_1, a_2 two constants independent of Δ. As we approach the transition $K \to K_c^-$, the gap Δ is expected to vanish, so we retain only the leading terms in the previous gap equation. This suggests distinguishing three cases depending on the sign of $2K_c - s$:

(1) $s - 2K_c > 0$: The gap equation reduces to $\Delta = a_1^{\frac{1}{2-4K}}$, which tells us that the critical point is $K_c = 1/2$ with $K < K_c$ corresponding to the gapped phase, while $K > K_c$ is gapless. We also understand that this gapped phase solution is valid only if $s > 2K_c = 1$, i.e., the bath is superohmic ($s > 1$).

(2) $s - 2K_c < 0$: Retaining only the leading terms yields $\Delta \sim a_2^{\frac{1}{2-s-2K}}$, signifying that $K_c = 1 - \frac{s}{2}$ and the gapped phase is for $K < K_c$. In this regime, $s < 2K_c = 2 - s$, which means the bath is subohmic ($s < 1$).

(3) $s - 2K_c = 0$: For K close to K_c, one expands $a^{2K-s} = 1 + (2K - s)\ln a$ since $2K - s \ll 1$, which shows that to

leading order $\Delta^{2-4K} \propto -\ln(\Delta\tau_c)$. This yields $K_c = 1/2$ and thus $s = 1$ which is an ohmic bath. This matches with the two previous cases but the gap is now discontinuous at the transition. This is a known artifact of the variational method [16,22].

In the spin chain picture, this gapped phase turns out to be an AFM. Indeed, by averaging Eq. (10) over all field configurations, one arrives at

$$\langle S_j^z \rangle = \frac{(-1)^{\frac{x_j}{a}}}{\pi} \langle \cos[2\phi(x_j)] \rangle, \quad (29)$$

which denotes the existence of an AFM phase with amplitude $\frac{1}{\pi}\langle \cos(2\phi) \rangle$. Using the variational propagator G_{AFM}^{-1} for the gapped phase, one then proves that $\langle \cos(2\phi) \rangle = (\Delta\tau_c)^K$, which can be obtained from the $\Delta\tau_c \ll 1$ limit of Eq. (H4). This implies that $\langle \cos(2\phi) \rangle$ can be used as an order parameter for this transition as this quantity vanishes in the LL and is finite in the AFM. Moreover, looking back at the gap expressions derived from the RG near the transition [$\Delta \sim \exp(-C(g-g_c)^p)$ or $\Delta \sim \exp(-C(\alpha-\alpha_c)^p)$], it appears that all derivatives of the order parameter vanish at the transition. This corroborates the scenario of a BKT-like phase transition which is known to be of infinite order. Physically, this order parameter is associated with the spontaneous symmetry breaking of the discrete shift symmetry $\phi(x,\tau) \rightarrow \phi(x,\tau) + \frac{n\pi}{2}$ of the bosonized field. Indeed, we expect $\langle \cos(2\phi) \rangle = \langle \cos(2\phi + \pi) \rangle = 0$ when the symmetry holds, which shows that the AFM is the symmetry-broken phase.

The fact this order parameter is associated with an AFM phase is not surprising as, in the case of a dissipative incommensurate spin chain, the ordered phase is a spin-density wave of wavelength π/k_F [13]. Putting $k_F = \frac{\pi}{2a}$, one recovers an AFM spin density wave with a $2a$ wavelength. All these results confirm the phase diagram obtained from the RG (see Fig. 2). There are two phases separated by $K_c = \max(1 - s/2, 1/2)$; for $K > K_c$, the system remains an LL, while for $K < K_c$ it becomes an AFM.

B. Phase diagram at finite coupling

In the previous subsection, we showed how the simple ansatz $G_{\text{AFM}}^{-1}(q, \omega_n) = \frac{1}{\pi K}[uq^2 + \frac{\omega_n^2}{u} + \frac{\Delta^2}{u}]$ was enough to capture the correct location of the phase transition when $\alpha, g \rightarrow 0$. However, from the RG results, we expect that starting at any value of $K > K_c$ and with g fixed, the system remains in the LL phase for $0 < \alpha < \alpha_c$ and switches to an AFM for $\alpha > \alpha_c$. At $\alpha = \alpha_c$, the system should be a LL with renormalized Luttinger parameter $K_r = K_c$. The same analysis is, of course, valid if tuning g while keeping α constant. One could therefore wonder if a more general ansatz $G_{\text{var}}^{-1}(q, \omega_n) = \frac{1}{\pi K_r}[u_r q^2 + \frac{\omega_n^2}{u_r} + \frac{\Delta_r^2}{u_r}]$, where u_r, K_r, Δ_r are fitting parameters to be determined, could capture the renormalization of the Luttinger parameters as predicted by the RG. It appears that this ansatz works well deep in the phase for finite α. However, it fails to recover the lowest order RG equations close to the transition (see Appendix F). In the next section, we will nonetheless use the respective renormalized quantities, denoted with a subscript r (e.g., the renormalized value of K is K_r and so on), as fitting parameters for our numerical analysis done at finite g, α.

VI. NUMERICAL RESULTS

In this section, we calculate different observables, both analytically and numerically, to observe the signature of the phase transition and physically characterize the ordered phase (AFM). For our numerical analysis, we simulate the Langevin dynamical equation for the field ϕ associated with the equilibrium probability distribution $P_{\text{eq.}}[\phi] = e^{-S[\phi]}$. The Langevin equation is $\frac{d\phi_{ij}(t)}{dt} = -\frac{\delta S[\phi_{ij}(t)]}{\delta \phi_{ij}(t)} + \eta_{ij}(t)$, where i, j are the discretized indices for imaginary-time τ and space x, respectively, t denotes the Langevin time (alternatively, the simulation time) and $\eta(t)$ is Gaussian white noise with $\langle \eta_{ij}(t) \rangle = 0$ and $\langle \eta_{ij}(t)\eta_{i'j'}(t') \rangle = 2\delta_{i,i'}\delta_{j,j'}\delta(t - t')$. Note that the noise η is used only for thermalizing the Langevin equation and is not to be confused with the noise coming from the dissipative bath, which has already been taken into account in the action $S[\phi]$. Using this numerical technique, we simulate configurations for fixed values of s, K and for different values of α. For each set of parameters, we extract field configurations of different sizes $L \times \beta$. We scale L as β, keeping the BKT dynamic scaling $z = 1$ in mind; and on these configurations, we calculate several observables to characterize the two phases. In the following, we show the results for $s = 0.5$ (subohmic bath), $K = 1$, $g = 0$, and $u = 1$. Results for $s = 1$ (ohmic bath) and $s = 1.5$ (superohmic bath) can be found in Appendix I.

A. Relevant observables

The first quantity that we calculate is the static susceptibility of the spin chain $\chi = \lim_{q \rightarrow 0}(q/\pi)^2 G(q, \omega_n = 0)$, also known as the compressibility of the field. Using the LL propagator $G_{\text{LL}} = \pi K_r[u_r q^2 + \frac{\omega_n^2}{u_r}]^{-1}$ derived in Sec. V, it appears that the static susceptibility is finite in the LL phase and is given by $\chi_{\text{LL}} = K_r/(u_r\pi)$. On the other hand, using $G_{\text{AFM}} = \pi K_r[u_r q^2 + \frac{\omega_n^2}{u_r} + \frac{\Delta_r^2}{u_r}]^{-1}$ shows that χ_{AFM} vanishes as $\frac{K_r u_r}{\Delta_r^2}q^2$ in the gapped phase and for $q \rightarrow 0$. These analytical predictions are then compared to the data from the Langevin simulation. Numerically, the Green's function $G(q, \omega_n)$ is obtained by computing the correlation function $\langle \phi(q, \omega_n)\phi(-q, -\omega_n) \rangle = \langle |\phi(q, \omega_n)|^2 \rangle$, as the fields are real and bosonic. The associated numerical results are depicted on the left of Fig. 4 and support our analytical predictions. In the LL ($\alpha = 1$), the quantity $\lim_{q \rightarrow 0}(q^2/\pi)G(q, \omega_n = 0) = \pi\chi$ is equal to $K_r/u_r = 1$ (top row). On the other hand, in the AFM ($\alpha = 5$), the $q \rightarrow 0$ limit vanishes (bottom row).

The next quantity that we calculate is given by $C(\omega_n) = \frac{1}{\pi L}\sum_{q=-\infty}^{\infty} G(q, \omega_n)$. In the thermodynamic limit, the sum over q can be replaced with the integral $\frac{1}{2\pi}\int_{-\infty}^{\infty} dq$. In this limit, using our variational action from Sec. V, we expect that for a small-ω_n limit,

$$C(\omega_n \rightarrow 0) = \begin{cases} \frac{K_r}{2\omega_n} & \text{LL} \\ \frac{K_r}{2\Delta_r}\left[1 - \frac{1}{2}\left(\frac{\omega_n}{\Delta_r}\right)^2\right] & \text{AFM}. \end{cases} \quad (30)$$

Comparing this to the numerical results in the middle of Fig. 4, we see that indeed for small α (LL phase), $\omega_n C(\omega_n)$ goes to a constant for $\omega_n \rightarrow 0$; whereas $C(\omega_n)$ itself saturates to a constant for a higher value of α (AFM phase), as
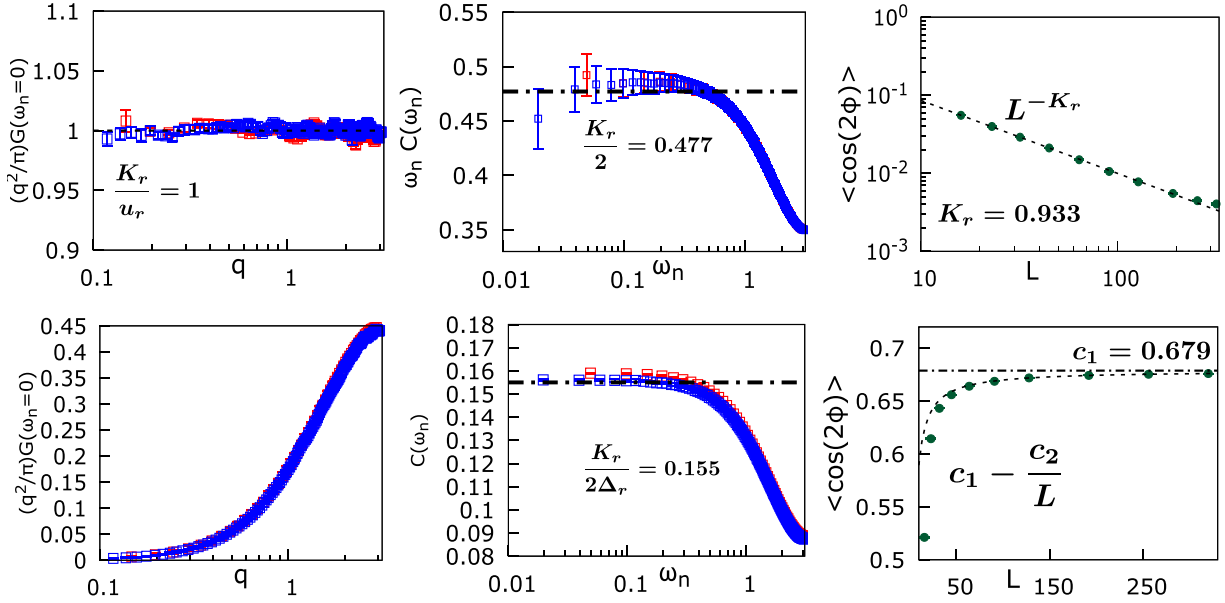
FIG. 4. Numerical evaluation of observables for the commensurate dissipative spin chain. The values of the parameters are taken to be $s = 0.5$, $K = 1$, $g = 0$, $u = 1$, and β is scaled as L. For the *left* and *middle* column, red and blue colors denote $L = 128$ and $L = 320$ respectively. All the quantities have been averaged over 10000-20000 configurations and the value of time-step dt is 0.5. (top) and (bottom) rows correspond to $\alpha = 1$ (LL) and $\alpha = 5$ (AFM), respectively. (left) Susceptibility χ as a function q. For $\alpha = 1$, it stays finite and constant whereas for $\alpha = 5$, it vanishes at small q. (middle) The behavior of $C(\omega_n)$ (Eq. 30) as a function of ω_n. For $\alpha = 1$, $\omega_n C(\omega_n)$ saturates to a constant $K_r/2 = 0.477$; for $\alpha = 5$, $C(\omega_n)$ becomes a constant $K_r/(2\Delta_r) = 0.155$. (right) Behavior of the order parameter $\langle \cos[2(\phi - \phi_{\text{CoM}})] \rangle$ as a function of system size L. For $\alpha = 1$, the order parameter decays as L^{-K_r} with $K_r = 0.933$, whereas for $\alpha = 5$, it increases and saturates to a constant as $c_1 - c_2/L$ with $c_1 = 0.679$ and $c_2 = 0.894$.

analytically predicted. This confirms the existence of a gap in the low-energy spectrum of the dissipative phase. One can also check the subleading ω_n dependence by numerically calculating $\frac{K_r}{2\Delta_r} - C(\omega_n)$. Figure 5 shows that this term varies as $\propto \omega_n^2$, which backs up our variational prediction of the absence of a fractional Laplacian term $|\omega_n|^s$.

Finally, we compute the order parameter $\langle \cos[2(\phi - \phi_{\text{CoM}})] \rangle$, where $\phi_{\text{CoM}} = \frac{1}{\beta L} \sum_{x,\tau} \phi(x, \tau)$ is the center of mass (CoM) of the configuration. The field has been offset by its
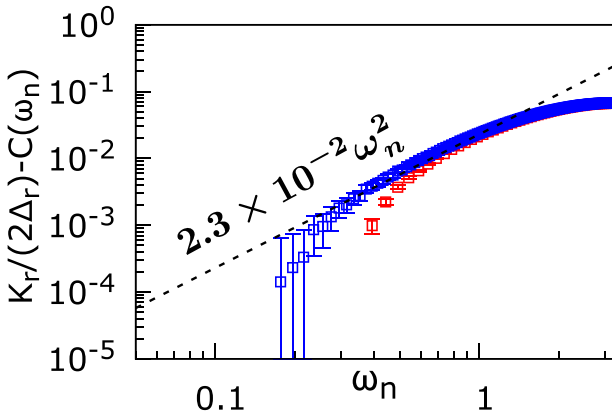

FIG. 5. $K_r/(2\Delta_r) - C(\omega_n)$ for the dissipative phase ($s = 0.5$, $K = 1$, $g = 0$, $\alpha = 5$). This quantity fits well with $2.3 \times 10^{-2}\omega_n^2$ for small ω_n, which is the subleading ω_n dependence of the propagator in the AFM. The red and blue colors denote two different system sizes $L = 128$ and $L = 320$, respectively.

CoM to suppress the contribution $G(0, 0)$ to the order parameter which would otherwise diverge in the gapless LL phase. In Appendix H, we analytically show that in the LL phase (with $\beta = L$), the order parameter vanishes as L^{-K_r}, whereas it increases and saturates to a constant in the AFM as $c_1 - c_2/L$, where c_1 and c_2 are both positive constants. Numerical results on the right of Fig. 4 corroborate this scenario. This confirms our prediction that the dissipative bath can induce a quantum phase transition on a 1D XXZ spin chain by spontaneously breaking the discrete shift symmetry $\phi \to \phi + \frac{n\pi}{2}, n \in \mathcal{Z}$, and the ordered phase is a gapped AFM phase.

B. Microscopic parameters

One can numerically extract relevant microscopic parameters in both phases from fitting the previous observables. In the LL phase, the relevant quantity is K_r, which can be extracted from the calculation of the order parameter by fitting it as a function of system size L (recall that it should scale as $\sim L^{-K_r}$), and from $C(\omega_n)$, which saturates to the constant $K_r/(2\Delta_r)$ as $\omega_n \to 0$. In the gapped phase, the extraction of the parameters is slightly more tricky as, at the lowest order, the quantitative behavior of the phase is regulated by the gap term. By computing $\lim_{q\to 0} \chi(q)/q^2$, one can nonetheless extract the value of the inverse of the gap $u_r K_r/\Delta_r^2$. The behaviors of these parameters are given in Fig. 6. From the plots, we see that K_r starts decreasing as α is increased and approaches $K_c = 0.75$ at the transition, after which Δ_r becomes finite and increases as α is increased. This tells us that for $K = 1$, $u = 1$, $g = 0$, and $s = 0.5$; the transition happens around $\alpha_c \in (2, 3)$.
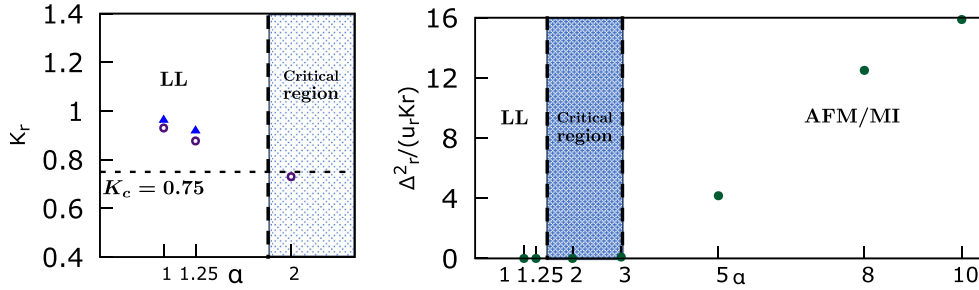
FIG. 6. Numerical phase diagram obtained for $K = 1$, $u = 1$, $g = 0$, $s = 0.5$ by varying α. Left: K_r in the LL phase as a function of α, extracted from the order parameter $\langle \cos[2(\phi - \phi_{\mathrm{CoM}})] \rangle$ (purple circles) and from $C(\omega_n)$ (blue triangles). K_r decreases to $K_c = 0.75$ as α is increased, signaling a BKT transition. Right: As α is increased, the gap (green dots) first becomes finite for $\alpha = 3$ and then increases.

VII. DISCUSSIONS AND CONCLUSIONS

In this paper, we investigated the zero-temperature properties of an XXZ spin chain at zero magnetization coupled to local baths of phonons à la Caldeira and Leggett [3]. Using the bosonization procedure, this system was mapped onto an effective field theory (with bosonic field ϕ), which could thus be tackled using powerful analytical and numerical field-theoretic tools. We confirmed the existence of a BKT-like phase transition between a LL exhibiting quasi-long-range order and an AFM phase with long-range order. The variational method predicts that the AFM does not present any fractional excitations as suggested by Ref. [16]. The exact location of the phase transition depends on the type of bath studied through the bath exponent s. For superohmic baths ($s > 1$), dissipation does not affect the transition which remains that of the isolated spin chain to the leading order. This transition is the standard BKT one. However, for subohmic baths ($s < 1$), the transition is shifted and the AFM eats into the LL. Although akin to the standard BKT universality class, this transition differs from the standard one. For subohmic baths, its location is shifted, while for ohmic baths the scaling of the gap near the transition is altered (see Sec. IV). It appears that, for all bath exponent s, the transition is associated with the spontaneous symmetry breaking of the order parameter $\langle \cos(2\phi) \rangle$. This quantity identifies with the amplitude of the antiferromagnetic spin density wave $S_j^z \sim (-1)^j \langle \cos(2\phi) \rangle$. As with a standard BKT transition, all derivatives of this order parameter vanish at the transition, signaling an infinite order phase transition.

While the variational method used in Sec. V successfully captured the main properties of both phases, it makes use of a rather crude approximation amounting to replacing the system's highly nonlinear action by a quadratic one. It is a well-established fact that such an approximate action fails at capturing topological excitations of the system such as solitons or instantons [22,37]. For a generic AFM with a vanishing linear conductivity, such excitations might lead to the restoring of nonlinear terms [38,39]. For our model, there are no instantons with finite action in the zero-temperature limit (see Chap. 3.2 of Ref. [37] for a proof of this statement), and the system is truly locked in one of the minima of the potential. Nonetheless, one might worry about the effect of solitons, for instance, on the transport properties, as for the pure sine-Gordon model. We leave for further investigation the understanding of this point. Moreover, the study of the

same model at finite temperature, where instantons connecting degenerate minima play an important role, seems an interesting path to explore.

Another direction we wish to explore is that of the competition between bath-induced localization, as studied in this paper and Refs. [12,13], and disorder-induced Anderson localization. One such example can be found in Ref. [40], where a quantum phase transition was found between an Anderson localized phase and a Zeno localized phase in a one-dimensional noninteracting system. Finally, valuable insights could probably be gained by mapping this system to a Coulomb-like gas using the general idea of the sine-Gordon to the 2D Coulomb gas mapping [41,42].

APPENDIX A: FIELD-THEORETICAL COUPLINGS FROM BOSONIZATION

The couplings K, u, g appearing in the bosonic field-theory in Eq. (12) are related to the microscopic parameters J_z, J_{xy}, a of the XXZ spin chain. Bosonization predicts the following correspondence:

$$K = \sqrt{1 + \frac{4J_z}{\pi J_{xy}}}^{-1}, \tag{A1}$$

$$u = aJ_{xy}\sqrt{1 + \frac{4J_z}{\pi J_{xy}}}, \tag{A2}$$

$$g = \frac{J_z}{J_{xy}}\sqrt{1 + \frac{4J_z}{\pi J_{xy}}}^{-1}, \tag{A3}$$

which is known to be valid in the regime $J_z \ll J_{xy}$. While an exact Bethe ansatz solution for the isolated XXZ spin chain exists [43], such a solution does not (yet) exist for the dissipative spin chain studied in this paper.

APPENDIX B: DISSIPATIVE KERNEL

When integrating out the bath degrees of freedom, one generates the dissipative kernel $\mathcal{D}(\tau, \tau') = \sum_k \mathcal{D}_k(\tau, \tau')$, where $\mathcal{D}_k^{-1}(\tau, \tau') = \frac{m_k}{\lambda_k^2} \delta(\tau - \tau')(\Omega_k^2 - \partial_\tau^2)$. To recover $\mathcal{D}_k(\tau, \tau')$, one must therefore invert $\mathcal{D}_k^{-1}(\tau, \tau')$, which amounts to finding $\mathcal{D}_k(\tau, \tau')$ such that

$$\int d\tau' \mathcal{D}_k(\tau, \tau') \mathcal{D}_k^{-1}(\tau, \tau') = \delta(\tau - \tau''). \quad \text{(B1)}$$

Using the following Fourier and inverse transform conventions:

$$\mathcal{D}_k(\omega, \omega') = \int d\tau d\tau' e^{i\omega\tau} \mathcal{D}_k(\tau, \tau') e^{-i\omega'\tau'}, \quad \text{(B2)}$$

$$\mathcal{D}_k(\tau, \tau') = \int \frac{d\omega}{2\pi} \frac{d\omega'}{2\pi} e^{-i\omega\tau} \mathcal{D}_k(\omega, \omega') e^{i\omega'\tau'}. \quad \text{(B3)}$$

Equation (B1) can be written in Fourier space as

$$\int d\omega' \mathcal{D}_k(\omega, \omega') \mathcal{D}_k^{-1}(\omega', \omega'') = 4\pi^2 \delta(\omega - \omega''). \quad \text{(B4)}$$

Let us apply this to the kernel $\mathcal{D}_k^{-1}(\tau, \tau')$. According to Eq. (B2), its Fourier transform is $\mathcal{D}_k^{-1}(\omega, \omega') = \frac{m_k}{\lambda_k^2} 2\pi \delta(\omega - \omega')(\Omega_k^2 + \omega'^2)$. From this expression and Eq. (B4), it is clear that $\mathcal{D}_k(\omega, \omega') = \frac{\lambda_k^2}{m_k} \frac{2\pi \delta(\omega - \omega')}{\Omega_k^2 + \omega'^2}$. This implies, along with Eq. (B3), that

$$\mathcal{D}_k(\tau, \tau') = \frac{\lambda_k^2}{m_k} \int \frac{d\omega}{2\pi} \frac{e^{-i\omega(\tau - \tau')}}{\Omega_k^2 + \omega^2} = \frac{\lambda_k^2}{2m_k\Omega_k} e^{-\Omega_k|\tau - \tau'|}. \quad \text{(B5)}$$

Performing the sum over k then yields

$$\mathcal{D}(\tau, \tau') = \int d\Omega \, e^{-\Omega|\tau - \tau'|} \sum_k \frac{\lambda_k^2}{2m_k\Omega_k} \delta(\Omega - \Omega_k), \quad \text{(B6)}$$

where we recognize the spectral function from Eq. (4) as $J(\Omega) = \frac{\pi}{2} \sum_k \frac{\lambda_k^2}{m_k\Omega_k} \delta(\Omega - \Omega_k) = \alpha \frac{\pi \Omega_D^{1-s}}{\Gamma(1+s)} \Omega^s$ for $\Omega \in [0, \Omega_D]$. This leads to

$$\mathcal{D}(\tau, \tau') = \alpha \frac{\Omega_D^{1-s}}{\Gamma(1+s)} \int_0^{\Omega_D} d\Omega \, \Omega^s e^{-\Omega|\tau - \tau'|}$$

$$= \frac{\alpha \Omega_D^{1-s}}{|\tau - \tau'|^{1+s}} \frac{\int_0^{\Omega_D|\tau - \tau'|} dx \, x^s e^{-x}}{\Gamma(1+s)}. \quad \text{(B7)}$$

For $|\tau - \tau'| \gg \tau_c = 1/\Omega_D$, one can approximate the integral as $\int_0^\infty dx \, x^s e^{-x} = \Gamma(1+s)$. Thus,

$$\mathcal{D}(\tau, \tau') = \frac{\alpha \tau_c^{s-1}}{|\tau - \tau'|^{1+s}}, \quad \text{(B8)}$$

which is the expression given in the main text.

APPENDIX C: PERTURBATIVE RG ANALYSIS

The goal of this Appendix is to compute the RG equations Eqs. (13)–(16) by means of the OPE.

1. Derivation of the useful OPEs

The OPE is a series expansion of a product of two nearby fields in terms of local fields. This is done on normal ordered operators to avoid any divergence not coming from the two operators being pushed together. For our problem, we will need the following OPEs:

$$: e^{2ip\phi(r)} :: e^{2ip\phi(r')} := a^{2p^2K} : e^{4ip\phi(r)} :, \quad \text{(C1)}$$

$$: e^{2ip\phi(r)} :: e^{-2ip\phi(r')} := \frac{: e^{2ip(\phi(r) - \phi(r'))} :}{|\delta r|^{2p^2K}}$$

$$= \frac{: 1 + 2ip\delta r \cdot \nabla\phi(r) - 2p^2(\delta r \cdot \nabla\phi(r))^2 :}{|\delta r|^{2p^2K}}, \quad \text{(C2)}$$

which imply

$$: \cos[2p\phi(r)] :: \cos[2p\phi(r')] := \frac{a^{2p^2K}}{2} : \cos[4p\phi(r)] :$$

$$- p^2 \frac{: (\delta r \cdot \nabla\phi(r))^2 :}{|\delta r|^{2p^2K}} + ..., \quad \text{(C3)}$$

$$: \cos[4\phi(r)] :: \cos[2\phi(r')] := \frac{: \cos[2\phi(r)] :}{2a^{4K}} + ... \quad \text{(C4)}$$

where $r = (x, u\tau)$, $r' = (x', u\tau')$, $\delta r = r' - r$. These relations are easily proven using the identity $: e^{i2p\phi(r)} := \frac{e^{i2p\phi(r)}}{\langle e^{i2p\phi(r)} \rangle} = \frac{e^{i2p\phi(r)}}{a^{p^2K}}$, where $\langle \cdot \rangle$ is the average with respect to the Gaussian action S_{LL}.

2. Renormalization group using the OPE

The interacting part of the action in Eq. (12) can be rewritten in terms of normal ordered fields as

$$S_{\text{int}} = S_g + S_\alpha$$

$$= -\frac{gu}{2\pi^2 a^{2-4K}} \int dx d\tau : \cos[4\phi(x, \tau)] :$$

$$- \frac{\alpha u^{1-s}}{2\pi^2 a^{2-s-2K}} \int_{|\tau - \tau'| > \tau_c} dx d\tau d\tau'$$

$$\times \frac{: \cos[2\phi(x, \tau)] :: \cos[2\phi(x, \tau')] :}{|\tau - \tau'|^{1+s}}. \quad \text{(C5)}$$

One then expands the partition function up to order $O(\alpha, g^2, \alpha g)$ such that

$$Z = \int \mathcal{D}\phi e^{-S_{\text{LL}}[\phi] - S_g[\phi] - S_\alpha[\phi]}$$

$$= Z_{\text{LL}} \left[1 - \langle S_g \rangle(a) - \langle S_\alpha \rangle(a) + \frac{\langle S_g^2 \rangle(a)}{2} + \langle S_\alpha S_g \rangle(a) \right], \quad \text{(C6)}$$

where the cutoff dependence has been made explicit. We now perform a rescaling of the lattice spacing $a \to a' = a(1 + dl)$ (so $\tau_c \to \tau_c' = \tau_c(1 + dl)$) and ask how the couplings should vary to preserve the partition function Z. Z_{LL} being an RG fixed-point, we only need to consider the variations of the averaged interacting terms. Keeping only the first order in dl, $\langle S_g \rangle(a')$ becomes

$$\langle S_g \rangle(a') = \langle S_g \rangle(a) \left[1 + \frac{dg}{g} + (4K - 2)dl \right]. \quad \text{(C7)}$$

The next term $\langle S_\alpha \rangle(a')$ requires a bit more work. We start by splitting the imaginary-time integral as $\int_{|\tau - \tau'| > \tau_c} [...] -$

$\int_{\tau_c' > |\tau - \tau'| > \tau_c} [\ldots]$. The first term is simply given by

$$\langle S_\alpha \rangle (a) \left[1 + \frac{d\alpha}{\alpha} + (2K + s - 2)dl \right], \qquad (C8)$$

while the second term, which involves only fields at very close positions, can be evaluated using the OPE (C3) and gives

$$dl \left[\frac{\alpha(a)u}{2\pi^2 a^{2-4K}} \int dx d\tau \langle : \cos[4\phi(x, \tau)] : \rangle \right.$$

$$\left. - \frac{\alpha(a)}{\pi^2 u} \int dx d\tau \langle : (\partial_\tau \phi(x, \tau))^2 : \rangle \right]. \qquad (C9)$$

The third term, namely, $\frac{1}{2}\langle S_g^2 \rangle(a')$, reads

$$\frac{\langle S_g^2 \rangle(a')}{2} = \frac{g^2 a'^{8K-4}}{8\pi^4} \int_{|r-r'|>a'} dr dr'$$

$$\times \langle : \cos 4\phi(r) :: \cos 4\phi(r') : \rangle. \qquad (C10)$$

For this term, one again splits the limits of the integral into $\int_{|r-r'|>a} dr dr' [\ldots] - \int_{a'>|r-r'|>a} dr dr' [\ldots]$. The first part is easily tractable, while the second requires the use of the OPE (C3). This yields

$$\frac{\langle S_g^2 \rangle(a')}{2} = \frac{\langle S_g^2 \rangle(a)}{2} \left[1 + \frac{2dg}{g} + (8K - 4)dl \right]$$

$$+ dl \frac{g^2}{2\pi^3} \int dr : (\nabla \phi(r))^2 :. \qquad (C11)$$

The last term $\langle S_g S_\alpha \rangle(a')$ can be, yet again, separated into a simple part and a part that requires the OPE (C4) to give

$$\langle S_g S_\alpha \rangle(a') = \langle S_g S_\alpha \rangle(a) \left[1 + \frac{dg}{g} + \frac{d\alpha}{\alpha} \right.$$

$$\left. + (6K + s - 4)dl \right] + dl \frac{g}{\pi} \langle S_\alpha \rangle(a). \qquad (C12)$$

Putting everything together, one arrives at

$$\langle S_g \rangle(a') + \langle S_\alpha \rangle(a') - \frac{\langle S_g^2 \rangle}{2}(a') - \langle S_g S_\alpha \rangle(a')$$

$$= \langle S_g \rangle(a) \left[1 + \frac{dg}{g} + (4K - 2)dl - \frac{\alpha}{g}dl \right]$$

$$+ \langle S_\alpha \rangle(a) \left[1 + \frac{d\alpha}{\alpha} + (2K + s - 2)dl - \frac{g}{\pi}dl \right]$$

$$- \frac{\langle S_g^2 \rangle(a)}{2} \left[1 + \frac{2dg}{g} + (8K - 4)dl \right]$$

$$- \langle S_g S_\alpha \rangle(a) \left[1 + \frac{dg}{g} + \frac{d\alpha}{\alpha} + (6K + s - 4)dl \right]$$

$$- dl \frac{\alpha(a)}{\pi^2 u} \int dx d\tau \langle : (\partial_\tau \phi(x, \tau))^2 : \rangle$$

$$- dl \frac{g^2}{2\pi^3} \int dr : (\nabla \phi(r))^2 :. \qquad (C13)$$

Upon imposing that the partition function Z remains unchanged, the RG equations for α and g can be directly read off. Those for K and u are found by re-exponentiating the remaining quadratic terms. In the end, one finds

$$\frac{d}{dl} \frac{u}{K} = \frac{g^2 u}{\pi^2}, \qquad (C14)$$

$$\frac{d}{dl} \frac{1}{uK} = \frac{2\alpha}{\pi u} + \frac{g^2}{\pi^2 u}, \qquad (C15)$$

$$\frac{d}{dl} g = (2 - 4K)g + \alpha, \qquad (C16)$$

$$\frac{d}{dl} \alpha = (2 - s - 2K)\alpha + \frac{g\alpha}{\pi}. \qquad (C17)$$

APPENDIX D: GAP CLOSURE IN THE OHMIC CASE

This Appendix derives the parameter p of the gap closure $\Delta \sim \exp(-Ct^{-p})$ in the ohmic case ($s = 1$), with t the distance in coupling space to the separatrix plane. The following derivation is based on Ref. [32].

1. Analytic derivation

To extract the behavior of the microscopic gap $\Delta(0)$ near the transition, one notices that the renormalized gap is simply $\Delta(l) = e^l \Delta(0)$ because of its scaling dimension. If one starts the RG flow in the dissipative phase, the couplings $g(l)$ and $\alpha(l)$ will become of order $O(1)$ after a renormalization time $l^\star$. This corresponds to a renormalized gap $\Delta(l^\star)$ of order $O(1)$, so $\Delta(0) \sim e^{-l^\star}$. The goal of the following argument is thus to extract this time $l^\star$.

Let us start from the RG Eqs. (13)–(16). Since $K_c = 1/2$ at $s = 1$, one sets $K = 1/2 + x$ to study the vicinity of the critical point. We also introduce $y_1 = g/\pi$ and $y_2 = \sqrt{\alpha/\pi}$. To leading order in x, y_1, y_2, the RG equations then read

$$\frac{d}{dl} x = -\frac{y_1^2 + y_2^2}{4}, \qquad (D1)$$

$$\frac{d}{dl} y_1 = -4x y_1 + y_2^2, \qquad (D2)$$

$$\frac{d}{dl} y_2 = -x y_2 + \frac{y_1 y_2}{2}, \qquad (D3)$$

where we have dropped the equation for u since it does not feedback into the other equations. Let us consider a trajectory starting near the separatrix (which is here a 2D manifold, see Fig. 7) and in the dissipative phase. Such a trajectory starts by shooting towards the origin (0,0,0), then drastically slows down near this point, and finally escapes towards $(-\infty, \infty, \infty)$. This corresponds to a capture time $l_1^\star$, followed by a transition time $l_2^\star$, and an escape time $l_3^\star$, which add up to a total dissipative time $l^\star = l_1^\star + l_2^\star + l_3^\star$.

From numerical simulations (see Fig. 7), it appears that all trajectories near the separatrix converge rapidly to a common line $\mathcal{L}_{\text{capture}}$. Plugging the ansatz $y_1 = m_1 x$ and $y_2 = m_2 x$ into Eqs. (D1)–(D3) shows that

$$\mathcal{L}_{\text{capture}} : y_1 = \frac{2}{3} x, \ y_2 = \frac{\sqrt{20}}{3} x. \qquad (D4)$$

Since y_1 and y_2 remain finite throughout this process, the time it takes to reach $\mathcal{L}_{\text{capture}}$ will be of order $O(t^0) \ll l^\star$ and the
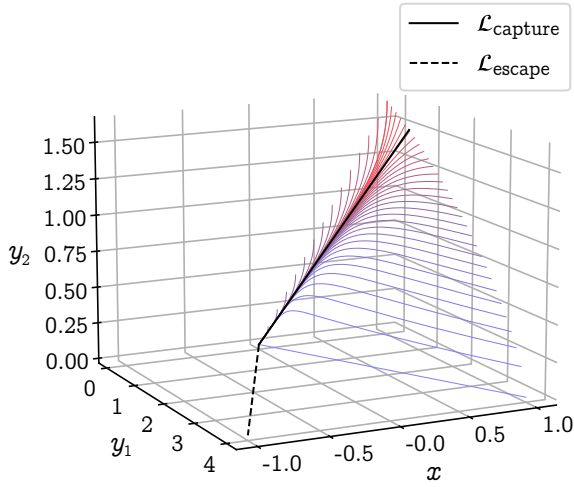
FIG. 7. The blue to red lines are trajectories which sit on the separatrix manifold between both phases. The large x side is the LL, while the small and negative x side is the AFM. All trajectories starting near the separatrix are quickly attracted to the the line $\mathcal{L}_{\text{capture}}$. Once they arrive near the origin, they tend to follow $\mathcal{L}_{\text{escape}}$.

distance t to the separatrix will only be rescaled by a finite prefactor. We can therefore assume that our trajectory starts at a point close to $\mathcal{L}_{\text{capture}}$ with a distance t to the separatrix. Once the trajectory has come close to the origin, it escapes along the line

$$\mathcal{L}_{\text{escape}} : y_1 = -4x, \quad y_2 = 0. \tag{D5}$$

a. Capture time. During the capture phase, the trajectory stays close to the capture line $\mathcal{L}_{\text{capture}}$, hence the notation $y_1 = \frac{2}{3}x + D_1$, $y_2 = \frac{\sqrt{20}}{3}x + D_2$, with D_1, D_2 the deviations from $\mathcal{L}_{\text{capture}}$. At leading order in the deviations, Eq. (D1) becomes

$$\frac{d}{dl}x = -\frac{2}{3}x^2 \Rightarrow x(l) = \frac{x_0}{1 + \frac{2x_0 l}{3}}, \tag{D6}$$

where we have set $x(l = 0) = x_0$. Equations (D2) and (D3) are then given to leading order by

$$\frac{d}{dl}\begin{pmatrix} D_1 \\ D_2 \end{pmatrix} = \frac{x}{9}\begin{pmatrix} -34 & 7\sqrt{20} \\ 5\sqrt{20}/2 & 4 \end{pmatrix}\begin{pmatrix} D_1 \\ D_2 \end{pmatrix}. \tag{D7}$$

Diagonalizing the 2×2 matrix shows that

$$\frac{d}{dl}\begin{pmatrix} D_+ \\ D_- \end{pmatrix} = x\begin{pmatrix} \lambda_+ & 0 \\ 0 & \lambda_- \end{pmatrix}\begin{pmatrix} D_+ \\ D_- \end{pmatrix}, \tag{D8}$$

with $\lambda_\pm = -\frac{5}{3} \pm \frac{\sqrt{79}}{3}$ and $D_\pm = \pm\frac{5}{6}\sqrt{\frac{5}{79}}D_1 + (\frac{1}{2} \pm \frac{19}{6\sqrt{79}})D_2$. Using Eq. (D6), the deviations $D_\pm$ are found to be

$$D_\pm(l) = D_\pm(l = 0)\left(1 + \frac{x_0 l}{2}\right)^{3\lambda_\pm/2}. \tag{D9}$$

Intuitively, D_- is the deviation from $\mathcal{L}_{\text{capture}}$ within the separatrix manifold while D_+ is the deviation outside of the manifold. Since, $\lambda_- < 0$ and $\lambda_+ > 0$, D_- quickly becomes negligible compared to D_+ and is therefore just dropped. Moreover, D_+ being the deviation from the separatrix, its initial condition is $D_+(l = 0) \sim t$.
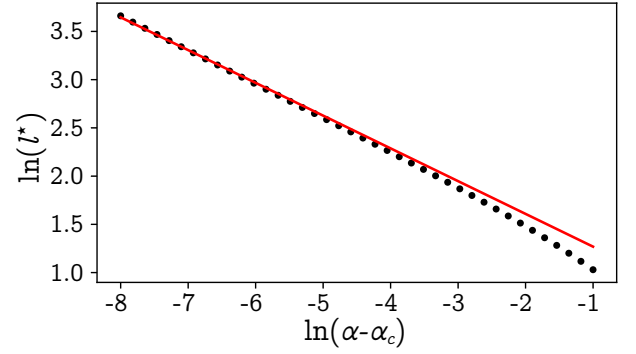

FIG. 8. Scaling of the total dissipative time $l^\star$ for trajectories starting close to the transition point α_c at $K = 1$ and $g = 0.5$. The dots are the numerical data points while the line is a fit using the ansatz $\ln(l^\star) = -0.3396 \times \ln(\alpha - \alpha_c) + C$.

The capture phase stops at a time $l_1^\star$ such that $D_+(l_1^\star) \sim x(l_1^\star)$. Using the expressions for $D_+(l)$ and $x(l)$ derived in Eqs. (D6) and (D9):

$$l_1^\star \sim t^{-\frac{1}{3\lambda_+/2+1}}. \tag{D10}$$

From the previous equations, it also follows that $x(l_1^\star) \sim D_+(l_1^\star) \sim 1/l_1^\star$.

b. Transition time. Starting at $l_1^\star$, the trajectory is stuck for some time $l_2^\star$ around the origin. During this time, y_1 and y_2 remain rather constant and x goes from $+x(l_1^\star)$ to $x(l_1^\star + l_2^\star) \sim -x(l_1^\star)$. Since $\frac{dx}{dl} = -(y_1^2 + y_2^2)/4 \sim -1/l_1^{\star 2}$ and $x(l_1^\star) \sim 1/l_1^\star$, this entire process takes a time $l_2^\star = 2x(l_1^\star)/(dx/dl) \sim l_1^\star$.

c. Escape time. For $l > l_{12}^\star = l_1^\star + l_2^\star$, the trajectory follows $\mathcal{L}_{\text{escape}}$. Looking at Eq. (D5), the adapted deviations are defined through $y_1 = -4x + D_1$, $y_2 = 0 + D_2$. To leading order, Eq. (D1) reduces to [recall that $x(l_{12}^\star) < 0$]

$$\frac{d}{dl}x = -4x^2 \Rightarrow x(l) = \frac{x(l_{12}^\star)}{1 + 4(l - l_{12}^\star)x(l_{12}^\star)}. \tag{D11}$$

The escape time is reached when $x(l)$ becomes of order $O(1)$, that is, when $l_3^\star = l^\star - l_{12}^\star \sim 1/x(l_{12}^\star)$, i.e., $l_3^\star \sim l_1^\star$.

Adding up $l_1^\star, l_2^\star, l_3^\star$ shows that $l^\star \sim t^{-p}$ with $p = \frac{1}{3\lambda_+/2+1} = \frac{\sqrt{79}+3}{35} \simeq 0.33966269\ldots$.

2. Numerical confirmation

The RG equations for K, g, α can be numerically integrated for any initial condition. For the initial values $K = 1$ and $g = 0.5$, we vary α to get close to the transition point α_c and measure the associated total dissipative time $l^\star$. This time is defined as the time needed for the simulation to reach the plane $K = 0.1$. The results are shown in Fig. 8. It appears that the data fits quite nicely with our ansatz $\ln(l^\star) = -0.3396 \times \ln(\alpha - \alpha_c) + C$ for $\alpha - \alpha_c \ll 1$.

APPENDIX E: GAP EQUATION FROM THE VARIATIONAL METHOD

We wish to find a solution to the self-consistent variational Eq. (26) using the following ansatz: $G_{\text{AFM}}^{-1}(q, \omega_n) =$

$\frac{1}{\pi K}[uq^2 + \frac{\omega_n^2}{u} + \frac{\Delta^2}{u}]$. Setting $\omega_n = q = 0$ in Eq. (26) yields

$$\frac{\Delta^2}{\pi K u} = \frac{8g}{\pi^2 a^2} \exp\left[-2K \int \frac{d\omega_n'}{\sqrt{\omega_n'^2 + \Delta^2}}\right]$$

$$+ \frac{4\alpha u^{-s}}{\pi^2 a^{2-s}} \int_{\tau_c}^{\infty} \frac{d\tau}{\tau^{1+s}} \exp\left[-K \int d\omega_n' \frac{1 + \cos\omega_n'\tau}{\sqrt{\omega_n'^2 + \Delta^2}}\right],$$

(E1)

where we have done both integrals over q in the exponentials. The remaining integrals over ω_n' are UV divergent and are regulated by reintroducing the imaginary-time cutoff $\tau_c = a/u$ (thus, $1/\tau_c$ in Matsubara frequency space). In the limit of $\Delta\tau \ll 1$, one can then find that $\int_0^{1/\tau_c} \frac{d\omega_n'}{\sqrt{\omega_n'^2 + \Delta^2}} = -\ln(\Delta\tau_c)$, and $\int_0^{1/\tau_c} d\omega_n' \frac{1 + \cos\omega_n'\tau}{\sqrt{\omega_n'^2 + \Delta^2}} = -\ln(\Delta^2\tau_c\tau) - \gamma_E$, with γ_E Euler's gamma constant. Plugging this back into Eq. (E1) gives

$$\frac{\Delta^2}{\pi K} = \frac{8g}{\pi^2 \tau_c^{2-4K}}\Delta^{4K} + \frac{4\alpha}{\pi^2 \tau_c^{2-s-2K}} \int_{\tau_c}^{\frac{1}{\Delta}} \frac{d\tau}{\tau^{1+s-2K}} \Delta^{4K} e^{2K\gamma_E},$$

(E2)

which, after doing the integral over τ and rearranging the terms, leads to

$$\frac{(\Delta\tau_c)^{2-4K}}{K} = g\frac{8}{\pi} + \alpha\frac{4e^{2K\gamma_E}}{\pi} \frac{(\Delta\tau_c)^{s-2K} - 1}{2K - s}.$$

(E3)

This is Eq. (28) in the text.

APPENDIX F: VARIATIONAL METHOD VS RG

This section shows how the ansatz $G_{\text{var}}^{-1}(q, \omega_n) = \frac{1}{\pi K_r}[u_r q^2 + \frac{\omega_n^2}{u_r} + \frac{\Delta^2}{u_r}]$ fails at predicting the correct renormalized coefficients close to the transition. For simplicity and to compare the result with the perturbative RG, we focus on the LL phase where $\Delta_r = 0$. Taking the second derivative with respect to q of Eq. (26) shows that $\frac{u_r}{K_r} = \frac{u}{K}$ so we can express both Luttinger parameters in terms of η such that $K = K_r\sqrt{1+\eta}$, $u = u_r\sqrt{1+\eta}$. The ansatz thus becomes $G_{\text{var}}^{-1}(q, \omega_n) = \frac{1}{\pi K}[uq^2 + \frac{\omega_n^2}{u}(1+\eta)]$, where η is the only parameter to solve for. Taking the second derivative of Eq. (26) with respect to ω_n yields

$$\eta = \frac{\alpha K}{\pi \tau_c^{2-s}} \int_{\tau_c}^{\infty} \frac{d\tau}{\tau^{-1+s}}$$

$$\times \exp\left[-\frac{K}{\pi} \int dq' d\omega_n' \frac{1 - \cos\omega_n'\tau}{uq'^2 + \frac{\omega_n'^2}{u}(1+\eta)}\right]. \quad (F1)$$

We now perform the integral over q and regulate the diverging integral over ω_n' by adding the imaginary-time UV cutoff τ_c to obtain

$$\eta = \frac{\alpha K}{\pi \tau_c^{2-s}} \int_{\tau_c}^{\infty} \frac{d\tau}{\tau^{-1+s}}$$

$$\times \exp\left[-2K_r \int_0^{1/\tau_c} d\omega_n' \frac{1 - \cos\omega_n'\tau}{\omega_n'}\right]. \quad (F2)$$
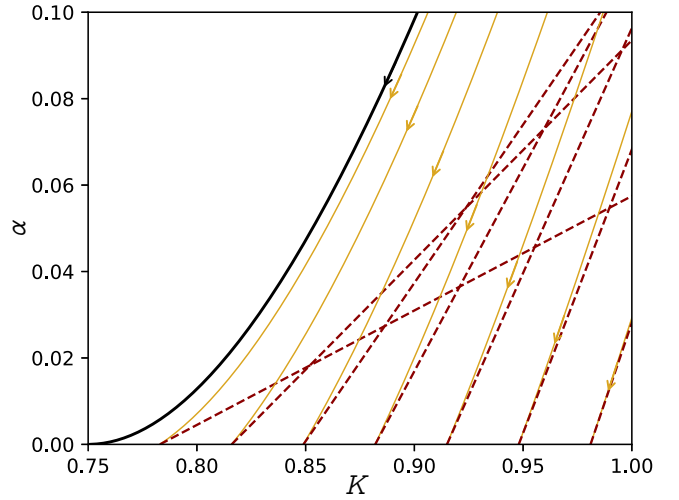

FIG. 9. RG flow in the LL phase of the couplings α and K according to the actual RG equations (solid gold lines) and the linearized equations (dashed red lines). This plot is for $s = 0.5$.

In the limit of large τ/τ_c, one proves the following identity:

$$\int_0^{1/\tau_c} d\omega_n' \frac{1 - \cos\omega_n'\tau}{\omega_n'} = \ln(\tau/\tau_c) + \gamma_E + O(\tau_c/\tau), \quad (F3)$$

which implies that

$$\eta = \frac{\alpha K e^{-2K_r\gamma_E}}{\pi \tau_c^{2-s-2K_r}} \int_{\tau_c}^{\infty} \frac{d\tau}{\tau^{-1+s+2K_r}}. \quad (F4)$$

Computing this integral and using $K = K_r\sqrt{1+\eta}$ leads to

$$\frac{\eta}{\sqrt{1+\eta}} = \frac{\alpha K_r e^{-2K_r\gamma_E}}{\pi(2K_r + s - 2)}. \quad (F5)$$

Now comes the problem. From the argument made in Sec. V, it is clear that the transition is given in terms of K_r by $(K_r)_c = \max(1 - s/2, 1/2)$. This means that for $s < 1$, Eq. (F5) predicts a renormalization of K and u that diverges towards the transition as

$$\sqrt{\eta} \simeq \frac{\alpha K_r e^{-2K_r\gamma_E}}{\pi(2K_r + s - 2)}, \quad (F6)$$

which is, of course, highly unphysical. This result can, however, be recovered from the RG using a very crude approximation: linearizing the RG flow about $\alpha = 0$ (see Fig. 9). To show how this recovers Eq. (F6), let us start by recalling the important RG equations for $s < 1$ (see Sec. IV C):

$$\frac{d}{dl}K = -\frac{\alpha K^2}{\pi}, \quad (F7)$$

$$\frac{d}{dl}\alpha = (2 - s - 2K)\alpha. \quad (F8)$$

In the LL phase, α flows to 0 and K to K_r. This means that K_r is given by $K_r = K + \int_K^{K_r} dK' = K + \int_\alpha^0 \frac{dK}{d\alpha}(\alpha')d\alpha'$. For the linearized RG flow shown in Fig. 9, $\frac{dK}{d\alpha}(\alpha') = \frac{dK}{d\alpha}(\alpha' = 0) = \frac{K_r^2}{\pi(2K_r+s-2)}$. Plugging this back into Eq. (F8) and using
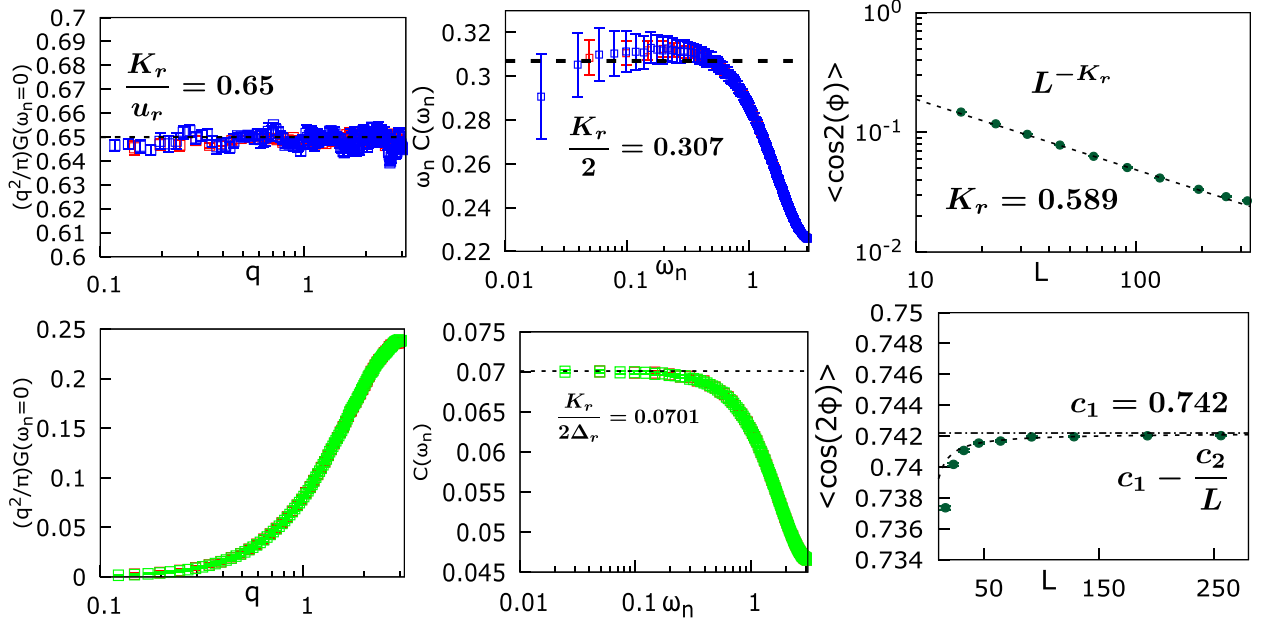
FIG. 10. Numerical evaluation of observables for the commensurate dissipative spin chain. The values of the parameters are taken to be $s = 1$ ($K_c = 0.5$), $K = 0.65$, $g = 0.5$, $u = 1$, and β is scaled as L. For the left and middle columns, red, green, and blue colors denote $L = 128$, $L = 256$, and $L = 320$, respectively. All the quantities have been averaged over 10 000–20 000 configurations and the value of time step dt is 0.5. (top) and (bottom) rows correspond to $\alpha = 0.5$ (LL) and $\alpha = 6$ (AFM), respectively. Left: Susceptibility χ as a function q. For $\alpha = 0.5$, it stays finite and constant, whereas for $\alpha = 6$ it vanishes for small q. Middle: Behavior of $C(\omega_n)$ as a function of ω_n. For $\alpha = 0.5$, $\omega_n C(\omega_n)$ saturates to a constant $K_r/2 = 0.307$; for $\alpha = 6$, $C(\omega_n)$ becomes a constant $K_r/(2\Delta_r) = 0.07$. Right: Behavior of order parameter $\langle\cos[2(\phi - \phi_{\text{CoM}})]\rangle$ as a function of system size L. For $\alpha = 0.5$, the order parameter decays as L^{-K_r} with $K_r = 0.59$, whereas for $\alpha = 6$, it increases and saturates to a constant as $c_1 - c_2/L$ with $c_1 = 0.742$ and $c_2 = 0.0296$.

$K = K_r\sqrt{1 + \eta}$ yields

$$\sqrt{1 + \eta} - 1 = \frac{\alpha K_r}{\pi(2K_r + s - 2)}. \tag{F9}$$

Near the transition ($K_r \to (1 - s/2)^+$), this equation becomes exactly Eq. (F6) up to the numerical factor $e^{-2K_r\gamma_E}$, which is probably an artifact of the approximation made in Eq. (F3). The main takeaway message is that the variational method captures the RG flow linearized about $\alpha = 0$, and thus breaks down close to the transition.

APPENDIX G: A SIMPLE ARGUMENT

In this Appendix, we show that the previous arguments allow to correctly capture the phase transition if the renormalisation of K is taken into account in a simpler manner, namely, without resorting to a self-consistent computation. This approximation should correspond to assuming that all the way down to $K_r = K_c$ the computation of K_r is perturbative in α. The computation amounts to replacing, in Eq. (F4), the value of K_r with K as

$$\eta = \frac{\alpha KC}{2\pi(K - K_c)}, \tag{G1}$$

with $C = e^{-2K\gamma_E}$, and then using η's definition

$$\eta = \left(\frac{K}{K_r}\right)^2 - 1, \tag{G2}$$

which, for $K_r = K_c$, recovers

$$(K - K_c)^2 \propto \alpha, \tag{G3}$$

which is the parabolic shape of the transition predicted by RG.

APPENDIX H: DERIVATION OF THE ORDER PARAMETER

In this Appendix, we show the calculation of the order parameter $\langle\cos(2(\phi - \phi_{\text{CoM}}))\rangle$ using our Gaussian variational ansatz. The behavior of this quantity in the LL has already been calculated in Ref. [13] [Appendix A shows that $\langle\cos(2(\phi - \phi_{\text{CoM}}))\rangle \propto L^{-K_r}$] so we concentrate on the AFM phase defined by the propagator $G_{\text{AFM}}(q, \omega_n) = \frac{1}{\pi K}(uq^2 + \frac{\omega_n^2}{u} + \frac{\Delta_r^2}{u_r})$. Since we work within our Gaussian variational theory, one writes $\langle\cos 2(\phi - \phi_{\text{CoM}})\rangle = \exp(-2\langle(\phi - \phi_{\text{CoM}})^2\rangle)$ where $\langle(\phi - \phi_{\text{CoM}})^2\rangle$ can be broken up as

$$\langle(\phi - \phi_{\text{CoM}})^2\rangle$$
$$= \frac{1}{\beta L}\left[\sum_{q \neq 0} G_{\text{AFM}}(q, 0)\right.$$
$$\left. + \sum_{\omega_n \neq 0} G_{\text{AFM}}(0, \omega_n) + \sum_{\omega_n \neq 0, q \neq 0} G_{\text{AFM}}(q, \omega_n)\right]. \tag{H1}$$
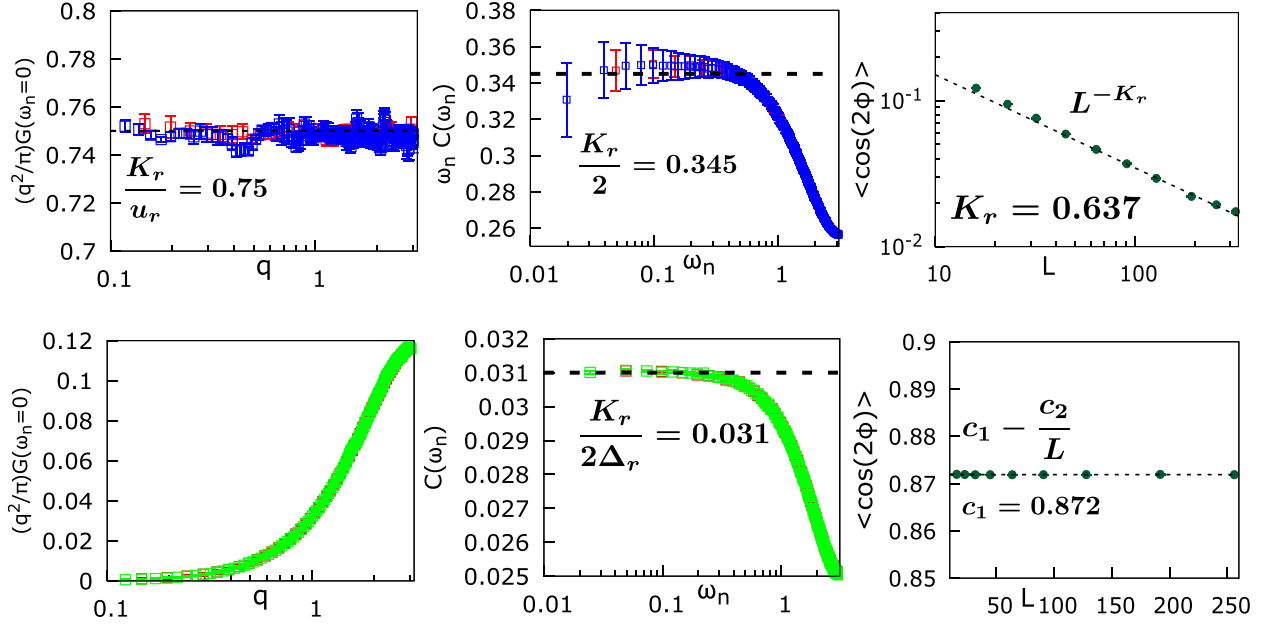
FIG. 11. Numerical evaluation of observables for the commensurate dissipative spin chain. The values of the parameters are taken to be $s = 1.5$ ($K_c = 0.5$), $K = 0.75$, $g = 1$, $u = 1$, and β is scaled as L. For the left and middle columns, red, green, and blue colors denote $L = 128$, $L = 256$, and $L = 320$, respectively, and β is scaled as L. All the quantities have been averaged over 10 000–20 000 configurations and the value of time step dt is 0.5. Top and bottom rows correspond to $\alpha = 0.65$ (LL) and $\alpha = 6$ (AFM), respectively. Left: Susceptibility χ as a function q. For $\alpha = 0.65$, it stays finite and constant whereas for $\alpha = 6$, it vanishes for small q. Middle: Behavior $C(\omega_n)$ as a function of ω_n. For $\alpha = 0.65$, $\omega_n C(\omega_n)$ saturates to a constant $K_r/2 = 0.345$; for $\alpha = 6$, $C(\omega_n)$ becomes a constant $K_r/(2\Delta_r) = 0.031$. Right: Behavior of order parameter $\langle \cos[2(\phi - \phi_{\text{CoM}})]\rangle$ as a function of system size L. For $\alpha = 0.65$, the order parameter decays as L^{-K_r} with $K_r = 0.637$, whereas for $\alpha = 5$ it increases and saturates to a constant as $c_1 - (c_2/L)$ with $c_1 = 0.872$ and $c_2 = 0$.

The first two terms can be computed for finite β and L using Matsubara sum techniques. This leads to

$$\sum_{q \neq 0} G_{\text{AFM}}(q, 0) = \frac{\pi K_r L}{2\Delta_r} \coth\left(\frac{\Delta_r L}{2u_r}\right) - \frac{\pi K_r u_r}{\Delta_r^2} \quad \text{(H2)}$$

and

$$\sum_{\omega_n \neq 0} G_{\text{AFM}}(0, \omega_n) = \frac{\pi K_r u_r \beta}{2\Delta_r} \coth\left(\frac{\Delta_r \beta}{2}\right) - \frac{\pi K_r u_r}{\Delta_r^2}. \quad \text{(H3)}$$

The third term is then replaced by its continuous limit ($L \to \infty$, $\beta \to \infty$) as the finite size effects are taken care of in the first two sums. Thus,

$$\frac{1}{\beta L} \sum_{\omega_n \neq 0, q \neq 0} G_{\text{AFM}}(q, \omega_n) = \frac{K_r}{4\pi} \int_{\sqrt{(u_r q)^2 + \omega_n^2} < \frac{1}{\tau_c}} d\omega_n dq \, \frac{1}{u_r q^2 + \frac{\omega_n^2}{u_r} + \frac{\Delta_r^2}{u_r}}$$

$$= -\frac{K_r}{4} \ln\left(\frac{(\tau_c \Delta)^2}{1 + (\tau_c \Delta)^2}\right), \quad \text{(H4)}$$

where we have introduced the UV cutoff τ_c. In our simulations, we take $L = \beta$ and then $L \to \infty$. Taking this same scaling, a large L expansion of the order parameter reads

$$\langle \cos(2(\phi - \phi_{\text{CoM}}))\rangle \simeq c_1 - \frac{c_2}{L} + \frac{c_3}{L^2}, \quad \text{(H5)}$$

where $c_1 = \left(\frac{\Delta \tau_c}{\sqrt{1 + (\Delta \tau_c)^2}}\right)^{K_r}$, $c_2 = c_1 \frac{\pi K_r}{\Delta_r}(1 + u_r)$, and $c_3 = c_1 \frac{\pi K_r}{\Delta_r^2}[4u_r + \pi K_r(1 + u_r)^2]$, respectively. We observe that the order parameter monotonically increases to a constant with a leading finite size dependence of $1/L$. This is a signature of the gapped phase, as a fractional phase would have finite size scaling $\propto L^{\frac{s}{2}-1}$, and a Luttinger liquid would have a $\propto L^{-K_r}$ behavior.

APPENDIX I: ADDITIONAL NUMERICAL RESULTS

In this Appendix, we provide additional numerical results that fortify the analytical claims made in the main text. As discussed in Sec. VI, we calculate the same correlation functions [χ, $C(\omega_n)$, and $\langle \cos[2(\phi - \phi_{\text{CoM}})]\rangle$] for ohmic and superohmic baths. The results are provided in Figs. 10 and 11, where numerical results are given for ohmic ($s = 1$) and superohmic ($s = 1.5$) baths, respectively, in a similar fashion as in Sec. VI. These plots confirm that the phase transition occurs for any value of $s \in (0, 2)$ and that the ordered phase is always an AFM phase. The values of the relevant simulation parameters and numerically extracted parameters are mentioned in the figure captions.

[1] P. W. Anderson, Absence of diffusion in certain random lattices, Phys. Rev. **109**, 1492 (1958).

[2] T. Maimbourg, D. M. Basko, M. Holzmann, and A. Rosso, Bath-induced Zeno localization in driven

many-body quantum systems, Phys. Rev. Lett. **126**, 120603 (2021).

[3] A. Caldeira and A. Leggett, Quantum tunnelling in a dissipative system, Ann. Phys. **149**, 374 (1983).

[4] A. J. Bray and M. A. Moore, Influence of dissipation on quantum coherence, Phys. Rev. Lett. **49**, 1545 (1982).

[5] A. J. Leggett, S. Chakravarty, A. T. Dorsey, M. P. A. Fisher, A. Garg, and W. Zwerger, Dynamics of the dissipative two-state system, Rev. Mod. Phys. **59**, 1 (1987).

[6] M. P. A. Fisher and W. Zwerger, Quantum Brownian motion in a periodic potential, Phys. Rev. B **32**, 6190 (1985).

[7] A. Schmid, Diffusion and localization in a dissipative quantum system, Phys. Rev. Lett. **51**, 1506 (1983).

[8] R. Nandkishore and D. A. Huse, Many-body localization and thermalization in quantum statistical mechanics, Annu. Rev. Condens. Matter Phys. **6**, 15 (2015).

[9] B. L. Altshuler, Y. Gefen, A. Kamenev, and L. S. Levitov, Quasiparticle lifetime in a finite system: A nonperturbative approach, Phys. Rev. Lett. **78**, 2803 (1997).

[10] D. A. Abanin, E. Altman, I. Bloch, and M. Serbyn, Colloquium: Many-body localization, thermalization, and entanglement, Rev. Mod. Phys. **91**, 021001 (2019).

[11] G. De Filippis, A. de Candia, L. M. Cangemi, M. Sassetti, R. Fazio, and V. Cataudella, Quantum phase transitions in the spin-boson model: Monte Carlo method versus variational approach à la Feynman, Phys. Rev. B **101**, 180408(R) (2020).

[12] S. Majumdar, L. Foini, T. Giamarchi, and A. Rosso, Bath-induced phase transition in a Luttinger liquid, Phys. Rev. B **107**, 165113 (2023).

[13] S. Majumdar, L. Foini, T. Giamarchi, and A. Rosso, Localization induced by spatially uncorrelated subohmic baths in one dimension, Phys. Rev. B **108**, 205138 (2023).

[14] M. A. Cazalilla, F. Sols, and F. Guinea, Dissipation-driven quantum phase transitions in a Tomonaga-Luttinger liquid electrostatically coupled to a metallic gate, Phys. Rev. Lett. **97**, 076401 (2006).

[15] Z. Cai, U. Schollwöck, and L. Pollet, Identifying a bath-induced Bose liquid in interacting spin-boson models, Phys. Rev. Lett. **113**, 260403 (2014).

[16] E. Malatsetxebarria, Z. Cai, U. Schollwöck, and M. A. Cazalilla, Dissipative effects on the superfluid-to-insulator transition in mixed-dimensional optical lattices, Phys. Rev. A **88**, 063630 (2013).

[17] T. Giamarchi and H. J. Schulz, Localization and interaction in one-dimensional quantum fluids, Europhys. Lett. **3**, 1287 (1987).

[18] T. Giamarchi and H. J. Schulz, Anderson localization and interactions in one-dimensional metals, Phys. Rev. B **37**, 325 (1988).

[19] E. V. H. Doggen, G. Lemarié, S. Capponi, and N. Laflorencie, Weak versus strong-disorder superfluid—Bose glass transition in one dimension, Phys. Rev. B **96**, 180202(R) (2017).

[20] B. Min, N. Anto-Sztrikacs, M. Brenes, and D. Segal, Bath-engineering magnetic order in quantum spin chains: An analytic mapping approach, arXiv:2401.06227.

[21] R. Citro, E. Orignac, and T. Giamarchi, Adiabatic-antiadiabatic crossover in a spin-Peierls chain, Phys. Rev. B **72**, 024434 (2005).

[22] T. Giamarchi, *Quantum Physics in One Dimension*, International Series of Monographs on Physics (Clarendon Press, Oxford, 2004).

[23] J. von Delft and H. Schoeller, Bosonization for beginners—refermionization for experts, Annalen der Physik **510**, 225 (1998).

[24] G. Giachetti, N. Defenu, S. Ruffo, and A. Trombettoni, Berezinskii-Kosterlitz-Thouless phase transitions with long-range couplings, Phys. Rev. Lett. **127**, 156801 (2021).

[25] G. Giachetti, A. Trombettoni, S. Ruffo, and N. Defenu, Berezinskii-Kosterlitz-Thouless transitions in classical and quantum long-range systems, Phys. Rev. B **106**, 014106 (2022).

[26] A. L. S. Ribeiro, P. McClarty, P. Ribeiro, and M. Weber, Dissipation-induced long-range order in the one-dimensional Bose-Hubbard model, arXiv:2311.07683.

[27] M. Weber, Quantum spin chains with bond dissipation, arXiv:2310.11525.

[28] A. M. Lobos, A. Iucci, M. Müller, and T. Giamarchi, Dissipation-driven phase transitions in superconducting wires, Phys. Rev. B **80**, 214515 (2009).

[29] Here and in the following, we call the BKT transition a transition whose RG equations are of the BKT type.

[30] J. Cardy, *Scaling and Renormalization in Statistical Physics*, Cambridge Lecture Notes in Physics (Cambridge University Press, Cambridge, 1996).

[31] N. Dupuis, Field Theory of Condensed Matter and Ultracold Gases, Vol. 2 (unpublished); https://www.lptmc.jussieu.fr/users/dupuis.

[32] D. R. Nelson, Study of melting in two dimensions, Phys. Rev. B **18**, 2318 (1978).

[33] J. L. Cardy, One-dimensional models with $1/r^2$ interactions, J. Phys. A: Math. Gen. **14**, 1407 (1981).

[34] Pushing the RG equations to higher orders shows that $\frac{d}{dl}\frac{u}{K} = O(\alpha^2)$. This is to be contrasted with the incommensurate spin chain [12,13] for which $\frac{d}{dl}\frac{u}{K} = 0$ is non-perturbative. This is because the system-bath interaction in the incommensurate spin chain action is invariant under the statistical tilt symmetry $\phi(x,\tau) \to \phi(x,\tau) + \mu x$, where μ is a constant.

[35] M. F. Maghrebi, Z.-X. Gong, and A. V. Gorshkov, Continuous symmetry breaking in 1D long-range interacting quantum systems, Phys. Rev. Lett. **119**, 023001 (2017).

[36] R. Feynman, *Statistical Mechanics: A Set of Lectures*, Frontiers in Physics (Sarat Book Distributors, Boca Raton, 1988).

[37] R. Rajaraman, *Solitons and Instantons: An Introduction to Solitons and Instantons in Quantum Field Theory*, North-Holland Personal Library (North-Holland Publishing Company, Amsterdam 1982).

[38] K. Maki, Soliton pair creation and low-temperature electrical conductivity of charge-density-wave condensates, Phys. Rev. B **18**, 1641 (1978).

[39] K. Hida and S. Nakaya, Quantum statistical mechanics of the sine-Gordon model with dissipation, in *Proceedings of the Yamada Conference XV on Physics and Chemistry of Quasi One-Dimensional Conductors*, edited by S. Tanaka and K. Uchinokura (Elsevier, Yamanashi, 1986), pp. 140–142.

[40] D. A. Huse, R. Nandkishore, F. Pietracaprina, V. Ros, and A. Scardicchio, Localized systems coupled to small baths: From Anderson to Zeno, Phys. Rev. B **92**, 014203 (2015).

[41] P. Minnhagen, The two-dimensional Coulomb gas, vortex unbinding, and superfluid-superconducting films, Rev. Mod. Phys. **59**, 1001 (1987).

[42] O. Bouverot-Dupuis, Mapping a dissipative quantum spin chain onto a generalized Coulomb gas, arXiv:2403.06618.

[43] F. D. M. Haldane, General relation of correlation exponents and spectral properties of one-dimensional Fermisystems: Application to the anisotropic $S = \frac{1}{2}$ Heisenberg chain, Phys. Rev. Lett. **45**, 1358 (1980).